

Temple University

Annual Progress Report: 2007 Formula Grant

Reporting Period

July 1, 2009 – June 30, 2010

Formula Grant Overview

The Temple University received \$1,957,901 in formula funds for the grant award period January 1, 2008 through December 31, 2011. Accomplishments for the reporting period are described below.

Research Project 1: Project Title and Purpose

Molecular Mechanisms of Calcium Entry in Cancer Cells - Numerous studies have identified altered Ca^{2+} signaling in cancer cells; recent work has led to the discovery and characterization of a previously unknown molecular regulator of Ca^{2+} signals named STIM1. Although cancer cells generally exhibit some changes in their Ca^{2+} responses, rhabdosarcoma cells exhibit loss of STIM1 expression; we propose to assess the impact of this on changes on Ca^{2+} signals, cancer cell growth and survival. This work will not only enhance our understanding of this specific type of cancer but may also lead to generally applicable new treatment strategies.

Duration of Project

7/1/2008 - 06/30/2010

Project Overview

An increase in cytosolic Ca^{2+} is a signaling component common to many different mitogens. Cytosolic Ca^{2+} is controlled through a combination of two closely linked processes – Ca^{2+} release from the endoplasmic reticulum (ER) and Ca^{2+} entry across the plasma membrane (PM). Numerous studies by our group and others have established that cancer cells exhibit differences in both their Ca^{2+} signaling systems, and their responses to changes in Ca^{2+} concentration. In particular, we have demonstrated that inhibition of Ca^{2+} entry in the presence of mitogens that stimulate Ca^{2+} release leads to apoptosis via a process we have termed Activation-Enhanced Cell Death. While the process of ER Ca^{2+} release is well understood, the different mechanisms of Ca^{2+} entry were, until recently, poorly described. However, recent studies have revealed that loss of ER Ca^{2+} content is sensed by the ER membrane protein STIM1, which activates a PM Ca^{2+} channel termed Orai1. Although expressed in most cell types, STIM1 expression is suppressed in rhabdosarcoma; these cells exhibit a unique sensitivity to STIM1 and die upon its expression. We are proposing a series of studies designed to define the relationship between expression of STIM proteins, Ca^{2+} entry signals and the formation of cancer cells. This will be achieved by altering expression levels of different regulators and mediators of Ca^{2+} signals and then assessing

the effect of these manipulations on the amount of Ca^{2+} entry, the rate of proliferation, sensitivity to different apoptotic pathways and potential crosstalk mechanisms between cytosolic Ca^{2+} concentration and these different pathways. Further, a series of studies have been designed based upon these principles to address the mechanism(s) involved in rhabdosarcoma STIM1 sensitivity. In addition to its important general implications towards the understanding of cancer cell biology and the regulation of Ca^{2+} entry, this work has specific implications towards the design of cancer treatment strategies, with significant potential to improve therapeutic outcome.

Principal Investigator

Jonathan Soboloff, PhD
Assistant Professor of Biochemistry
Temple University
Kresge Building, Rm. 624
Temple University School of Medicine
3440 N. Broad St.
Philadelphia, PA 19140

Other Participating Researchers

Yandong Zhou, PhD - employed by Temple University

Expected Research Outcomes and Benefits

Many hormones and factors signal changes in cell function through changes in the concentration of intracellular calcium. In different contexts, this can regulate cell growth, proliferation, cell death or cell differentiation. Prior work by us and others has shown that many types of cancer have altered calcium signals. However, since the proteins that regulate calcium signals were, until quite recently, poorly described, calcium is not a current therapeutic target. Recent work by us and others has led to the discovery and characterization of previously unknown molecular regulators of calcium signals known as STIM proteins. Importantly, rhabdosarcoma cells exhibit altered expression of STIM proteins, although their calcium signals have not been studied. We propose to study the relationship between calcium signals and cancer cell growth and survival, focusing primarily on STIM-mediated calcium signals. This will be done primarily by changing the levels of expression of STIM proteins and then determining how this impacts on calcium signals, rates of proliferation, sensitivity to cell death signals and other signaling components of these pathways. Completion of this work will not only enhance our understanding of these types of cancer but may ultimately lead to improved strategies for therapeutic intervention.

Summary of Research Completed

Aim 1: To characterize Ca^{2+} signaling systems in G401 rhabdosarcoma cell lines.

(i) Determination and manipulation of Ca^{2+} channel expression in rhabdosarcoma

(a) In order to determine the identities of the major SOC proteins in G401 cells, the levels of expression of each member of the STIM and Orai families were determined by qPCR (Fig 1A) and Western analysis (when possible; Fig 1B). HEK293 cells, a well characterized cell line with

similar morphology were used to compare STIM and Orai expression levels. Interestingly, all 5 members of the STIM and Orai families were expressed in both cell lines, although differences did exist in their relative levels of expression. Hence, G401 cells exhibited greater STIM2 than STIM1 expression (both at the RNA and protein levels) whereas the opposite was true in HEK293 cells. Further, G401 cells exhibited higher expression of each of the 3 members of the Orai family than HEK293 cells. This information has provided us with an essential starting point for the characterization of the store-operated Ca^{2+} signaling pathways in G401 cells.

(b) To determine the relative levels of expression of each member of the TRPC channel family in G401 cells, qPCR was used (Fig 2). Primers were designed using Premier Primer 5.0 and specificity was determined by BLAST. We found that TRPC1, TRPC4 and TRPC6 are the predominant TRPC channels expressed in this cell type. In contrast TRPC3, TRPC5 and TRPC7 expression levels were negligible. TRPC2 expression was not examined as this channel is a pseudogene in primates. This information provides us with a critical baseline to characterize Ca^{2+} signaling pathways in G401 cells.

(c) Although we have had considerable success using electroporation and lipofectamine for transfecting cell lines, viral approaches can be highly advantageous, particularly for studies of primary cells, either in vitro or in vivo. Therefore, we attempted to generate retroviral and adenoviral constructs to manipulate the expression of STIM1, STIM2 and Orai1. To generate STIM and Orai shRNA viruses we obtained a series of retroviral shRNA constructs targeting each gene and tested their abilities to inhibit STIM and Orai expression using either Western analysis (Fig 3A) or functional studies (Fig 3B). Unfortunately, multiple attempts to generate retroviruses from these vectors were unsuccessful for reasons unknown. Nevertheless, since these constructs contain an 'LTR' sequence for integration into the genome, they remain useful tools that can be used to stably knockdown STIM or Orai1 expression.

Unlike our attempts at generating retrovirus, we were successful in making infective adenovirus containing STIM1, STIM2 or Orai1 (Fig 3). While they are capable of infecting virtually any cell type, for safety reasons, these adenoviruses are replication-deficient since they lack the capacity to generate functional new viruses and, therefore, these infections cannot spread. To overcome this deficiency in the adenoviral genome, adenoviral-transformed AD293 cells were transfected with linearized replication-deficient adenoviral vectors. As these cells stably expressed the missing components, successful production of infectious STIM1-, STIM2- or Orai1-expressing adenovirus resulted as demonstrated by our successful test in G401 cells (Fig 3C).

(ii) To examine Ca^{2+} responses in rhabdomyosarcoma.

(a) *Store-operated Ca^{2+} signals:* In our original proposal, we stated a plan to simultaneously add thapsigargin and Cch in the presence or absence of extracellular Ca^{2+} . Unfortunately, in preparing to complete this experiment, we discovered that G401 cells do not have muscarinic receptors and therefore do not respond to Cch (discussed further in the subsequent subsection. As such, this experiment became impractical to complete. However, we were able to measure SOCE using our standard approach, exposure to the ER Ca^{2+} pump inhibitor thapsigargin (Tg; Fig 4). Intriguingly, we found that this pathway is constitutively activated, in that we observed significant Ca^{2+} entry prior to the addition of Tg. A manuscript based largely on our subsequent characterization of this observation and its significance is currently being considered for publication by the journal *Cell Death Differ*.

(b) *Receptor-operated Ca²⁺ signals*: Unfortunately, we were unable to identify any agonist capable of inducing receptor-mediated calcium entry in G401 cells, despite examining not only Cch and EGF, but also, bradykinin and caffeine (Fig 5). As such, this experiment could not be completed.

Aim 2: To characterize the importance of the STIM1 deletion in rhabdosarcoma

(i) *Loss of STIM1 is required for rhabdosarcoma survival.* The details of this completed sub-aim were provided in June 2009 report.

(ii) *Titration of STIM1 into rhabdosarcoma cells.* The details of this completed sub-aim were provided in June 2009 report.

(iii) *Characterization of Ca²⁺ signals in rhabdosarcoma cells.* The details of this completed sub-aim were provided in June 2009 report.

(iv) *Characterization of cell death in rhabdosarcoma cells.* In section 2(i) of our June 2009 report, we showed that STIM2 overexpression in G401 cells resulted in cell death. Since STIM2 dramatically increased constitutive Ca²⁺ entry in this cell type, the obvious implication is that they died from mitochondrial Ca²⁺ overload. Therefore, our efforts to characterize STIM2-induced cell death in G401 cells focused on the mitochondria. As depicted in figure 6A, visualization of mitochondria by transfecting G401 cells with mitochondrial dsRed revealed a typical filamentous pattern. While co-transfection with STIM1 had no effect on mitochondrial morphology (Fig 6B), mitochondria in STIM2-expressing cells were bloated and fragmented (Fig 6C). These observations indicate that STIM2-induced cell death in G401 cells results from mitochondrial Ca²⁺ overload, and not from ER stress or a general enhancement to apoptosis, the alternative pathways we considered in our original proposal.

(v) *Role of STIM2 in rhabdosarcoma.* The details of this completed sub-aim were provided in June 2009 report.

(vi) *Overexpression of TRPC3 in rhabdosarcoma.* In an effort to determine if G401 cells would fail to tolerate store-independent Ca²⁺ entry signals, we overexpressed TRPC3 (a Ca²⁺ permeant, receptor-operated cation channel). Cells were then stained with a fluorescent form of Annexin-V which binds phosphatidyl serine, a plasma membrane phospholipid found only on the inner half of the membrane in healthy cells. During apoptosis, failure to properly regulate the normal topology of the plasma membrane causes the appearance of phosphatidyl serine on both sides of the membrane. Annexin fluorescence levels were determined by flow cytometry. As expected, minimal Annexin staining could be detected in untreated G401 cells (significant Annexin staining was observed in 0.9% of cells). In TRPC3-overexpressing G401 cells, this number increased to 4.3%. While a somewhat marginal effect, this result is consistent with the idea that G401 cells have limited tolerance to Ca²⁺ entry, irrespective of whether it is store-dependent or – independent.

FIGURES

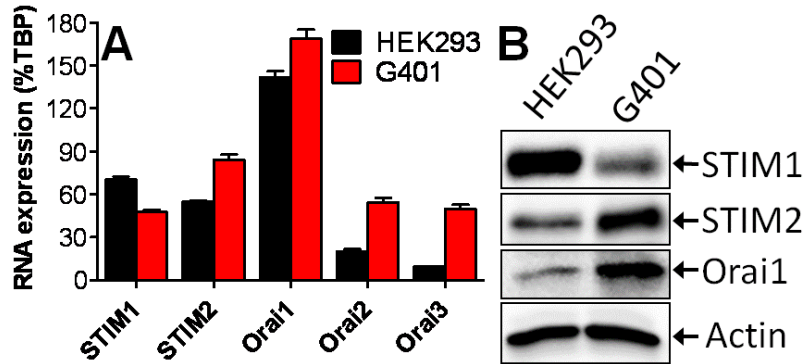


Fig 1: G401 cells exhibit decreased STIM1, but increased STIM2 expression. (A) G401 and HEK293 cells were analyzed for expression of all members of the STIM and Orai families by qPCR. Data were normalized to TATA-binding protein (TBP). Note that analysis of the dissociation curves revealed single peaks for all PCR products. (B) Expression of STIM1, STIM2 and Orai1 in G401 and HEK293 determined by Western blot. Actin was used as a loading control.

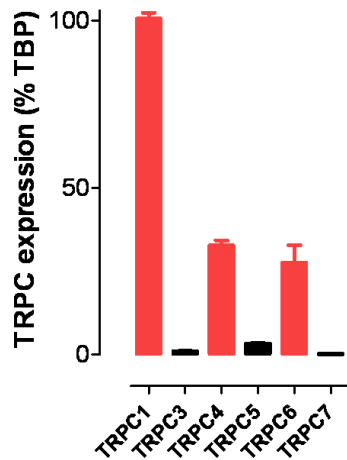


Fig. 2. Expression pattern of TRPC channels in G401 cells. G401 cells were lysed and analyzed for TRPC channel expression patterns by qPCR. Data were normalized to TATA-binding protein (TBP). Note that analysis of the dissociation curves revealed single peaks for all PCR products.

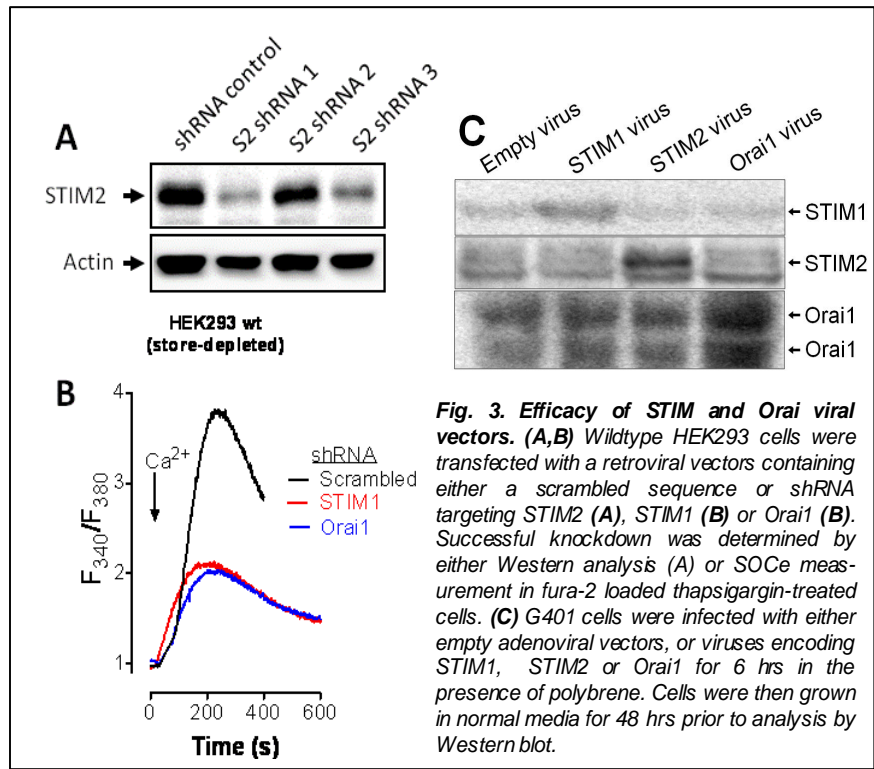


Fig. 3. Efficacy of STIM and Orai viral vectors. (A,B) Wildtype HEK293 cells were transfected with a retroviral vectors containing either a scrambled sequence or shRNA targeting STIM2 (A), STIM1 (B) or Orai1 (B). Successful knockdown was determined by either Western analysis (A) or SOCe measurement in fura-2 loaded thapsigargin-treated cells. (C) G401 cells were infected with either empty adenoviral vectors, or viruses encoding STIM1, STIM2 or Orai1 for 6 hrs in the presence of polybrene. Cells were then grown in normal media for 48 hrs prior to analysis by Western blot.

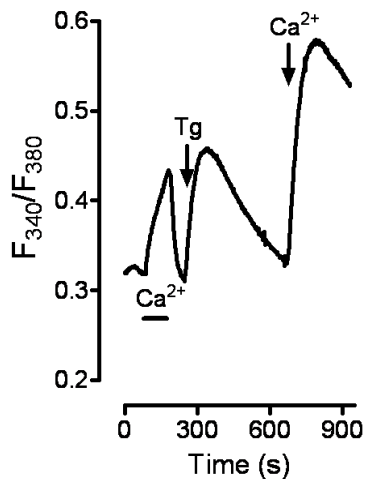


Fig. 4. SOCE measurement in G401 cells. SOCE was measured in fura-2 loaded G401 cells use fluorescence microscopy.

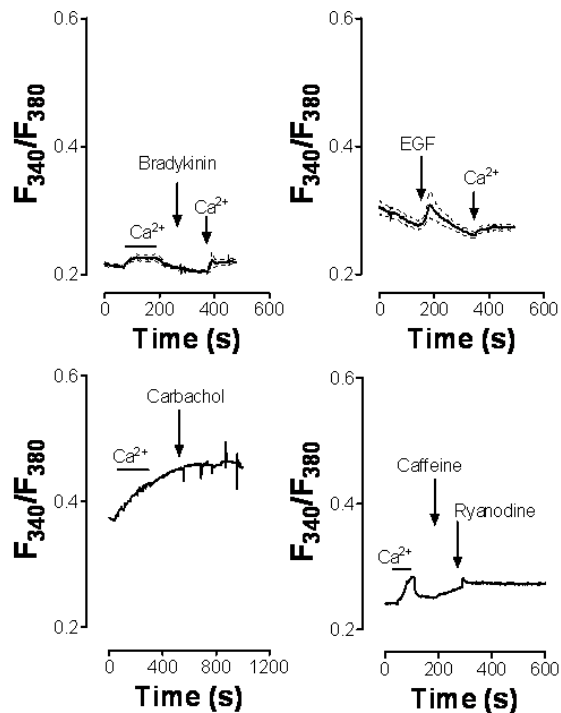


Fig. 5. Lack of agonist-induced Ca²⁺ responses in G401 cells. G401 cells were loaded with fura-2 and exposed to each of Bradykinin, EGF, Carbachol, Caffeine and ryanodine to determine if they would stimulate Ca²⁺ responses use fluorescence microscopy.

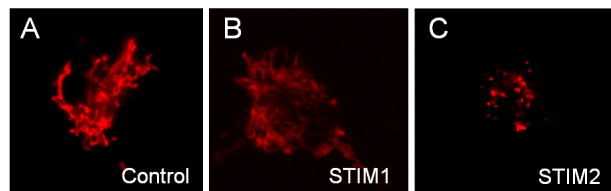


Fig. 6. Sensitivity of G401 cells to STIM2 overexpression. Cells were co-transfected with Mito-DSRed and either YFP (A), YFP-STIM1 (B), or YFP-STIM2 (C) and incubated for 48 hrs.

Research Project 2: Project Title and Purpose

Characterization of Transcriptional Elements Controlling Expression of DDH1 in Lung and Liver Cancer Cells - Dihydrodiol dehydrogenases (DDH) are a family of aldo-keto reductases involved in the de novo detoxification of xenobiotics. Expression profiles have indicated increased expression of DDH1 in human lung, liver and esophageal tumors as well as in carboplatin- and cisplatin-resistant human ovarian and lung cancer cells. This increase in DDH protein expression was associated with the alterations in the transcription of the DDH gene suggesting that the promoter region of the DDH gene plays an important role in controlling its expression. This study aims to decipher the precise genetic elements and its associated transcription factor(s) that control the induction of DDH1 gene in human lung and liver cancer cells. Identification of the transcriptional controls of DDH expression will allow designing strategies to control its expression and thus interfere with the process of carcinogenesis as well as development of tumor cell resistance to anticancer drugs.

Anticipated Duration of Project

7/1/2008 - 6/30/2009

Summary of Research Completed

This project ended during a prior state fiscal year. For additional information, please refer to the Commonwealth Universal Research Enhancement Annual C.U.R.E. Reports on the Department's Tobacco Settlement/Act 77 web page at <http://www.health.state.pa.us/cure>.

Research Project 3: Project Title and Purpose

Mercury-Induced Cell Death: a Source of Autoantigen? - Recent work in the field of autoimmunity has focused on apoptotic cells as a possible source of autoantigen. In the setting of murine mercury-induced autoimmunity, mercury-induced cell death, which differs from apoptosis, may be the source of autoantigen. This study will aim to characterize the Hg-induced cell death process and its effects on fibrillarin, the self antigen most specifically targeted in murine Hg-induced autoimmunity.

Duration of Project

7/1/2008 - 6/30/2009

Summary of Research Completed

This project ended during a prior state fiscal year. For additional information, please refer to the Commonwealth Universal Research Enhancement Annual C.U.R.E. Reports on the Department's Tobacco Settlement/Act 77 web page at <http://www.health.state.pa.us/cure>.

Research Project 4: Project Title and Purpose

Inhibition of HIV Infection Targeting cFMS Signaling Pathways - Once infected with HIV, cells known as tissue macrophages are resistant to the effects of current drugs that are used to treat HIV infection. Infected macrophages likely exert detrimental effects on the immune system and contribute to neurologic abnormalities associated with HIV infection. The studies proposed here investigate pathway(s) whereby HIV infection, by its upregulation of Macrophage Colony Stimulating Factor production in the infected cell, orchestrates the long-term survival of the infected macrophages. The studies should help develop strategies that can be used to help eliminate virus infected cells and help to clear HIV infection in combination with current therapies.

Duration of Project

7/1/2008 - 6/30/2009

Summary of Research Completed

This project ended during a prior state fiscal year. For additional information, please refer to the Commonwealth Universal Research Enhancement Annual C.U.R.E. Reports on the Department's Tobacco Settlement/Act 77 web page at <http://www.health.state.pa.us/cure>.

Research Project 5: Project Title and Purpose

Mechanism of JCV Involvement in Brain Tumors - The human polyomavirus, JCV, infects greater than 80% of the human population worldwide and remains in a latent state throughout life. Under certain physiological conditions such as immunosuppression, JCV becomes reactivated and induces the fatal demyelinating disease, progressive multifocal leukoencephalopathy (PML) in the brain. In addition, JCV has been shown to possess oncogenic activity in several experimental animals and has been detected in a significant number of human brain tumors including medulloblastomas and glioblastomas. The purpose of this study is to unravel the underlying molecular events associated with tumorigenesis of JCV and translate the knowledge from these studies toward the development of therapeutic strategies.

Duration of Project

7/1/2008 - 6/30/2009

Summary of Research Completed

This project ended during a prior state fiscal year. For additional information, please refer to the Commonwealth Universal Research Enhancement Annual C.U.R.E. Reports on the Department's Tobacco Settlement/Act 77 web page at <http://www.health.state.pa.us/cure>.

Research Project 6: Project Title and Purpose

Immune Regulation and Reactivation of JC Virus in the Demyelinating Disease, PML - Progressive multifocal leukoencephalopathy (PML) is a fatal demyelinating disease caused by JC virus which has recently occurred in patients with autoimmune disorders being treated with the powerful immunosuppressive therapy, rituximab. Our project will lay a foundation for determining the mechanisms involved in immune regulation of JC virus and investigate how rituximab may promote JC virus infection through soluble immunomodulators.

Duration of Project

7/1/2008 - 6/30/2009

Summary of Research Completed

This project ended during a prior state fiscal year. For additional information, please refer to the Commonwealth Universal Research Enhancement Annual C.U.R.E. Reports on the Department's Tobacco Settlement/Act 77 web page at <http://www.health.state.pa.us/cure>.

Research Project 7: Project Title and Purpose

The Role of ICOS in Mercury-Induced Autoimmunity - An inducible co-stimulatory molecule (ICOS) is a molecule expressed on the surface of white blood cells. It plays an important role in the immune response and blocking antibodies to ICOS are promising new treatments for conditions such as autoimmune diseases. We want to understand the role of ICOS in a mouse model of heavy metal-induced autoimmune disease and to fully assess its role as a potential therapeutic target.

Duration of Project

7/1/2008 - 6/30/2009

Summary of Research Completed

This project ended during a prior state fiscal year. For additional information, please refer to the Commonwealth Universal Research Enhancement Annual C.U.R.E. Reports on the Department's Tobacco Settlement/Act 77 web page at <http://www.health.state.pa.us/cure>.

Research Project 8: Project Title and Purpose

Role of Excess Ca²⁺ Influx in Cardiac Dysfunction after Myocardial Infarction - Congestive heart failure (CHF) is a devastating syndrome with 50% mortality within five years. It develops after the heart is challenged with hemodynamic stress imposed by hypertension, cardiac attack and genetic alterations. The current view on CHF is that the myocyte (heart cell), the basic component responsible for heart contraction, is weaker than normal. In contrast, there is an emerging concept that the loss of working heart cells plays a critical role in the progression of

CHF. In this study, we will use a transgenic mouse model with heart specific overexpression of the L-type calcium channel (Cav1.2) to determine whether the increase of contractility by overexpressing Cav1.2 will rescue heart failure induced by myocardial infarction (heart attack) or worsen CHF development by inducing myocyte loss.

Duration of Project

9/16/2008 – 6/30/2009

Summary of Research Completed

This project ended during a prior state fiscal year. For additional information, please refer to the Commonwealth Universal Research Enhancement Annual C.U.R.E. Reports on the Department's Tobacco Settlement/Act 77 web page at <http://www.health.state.pa.us/cure>.

Research Project 9: Project Title and Purpose

Loss of Wilms' Tumor Suppressor 1 Regulates STIM1-mediated Ca²⁺ Entry - Wilms' Tumor is one of the most common pediatric tumors, occurring 1/10,000 people in North America. It is thought to result from the loss of a transcriptional regulator known as Wilms' Tumor Suppressor 1 (WT1). Preliminary studies in our laboratory have linked WT1 with a Ca²⁺ entry pathway known as store-operated Ca²⁺ entry. This is important, because changes in Ca²⁺ concentration are linked to cell growth, differentiation and cell death. Hence, our goal is to gain a better understanding of Ca²⁺ signals, how the loss of WT1 causes Wilms' Tumor and how to design new treatment strategies.

Duration of Project

9/16/2008 – 6/30/2009

Summary of Research Completed

This project ended during a prior state fiscal year. For additional information, please refer to the Commonwealth Universal Research Enhancement Annual C.U.R.E. Reports on the Department's Tobacco Settlement/Act 77 web page at <http://www.health.state.pa.us/cure>.

Research Project 10: Project Title and Purpose

The Role of Osteoactivin in Osteoblast Development and Function - Osteoactivin (OA) has recently emerged as an important factor in osteogenesis. The identification of novel anabolic agents in bone and, perhaps even more importantly, gaining insights into their mechanisms of action, are subjects of intense clinical interest. Systemic or localized forms of bone loss are caused by a variety of diseases or conditions, including aging, and the resulting osteopenia is accompanied by an increased incidence of fracture. Treatment of patients with osteoporosis is a major health care challenge and many pharmaceutical companies are focused on identifying novel therapeutic agents that can selectively stimulate new bone formation.

Duration of Project

9/16/2008 – 6/30/2009

Summary of Research Completed

This project ended during a prior state fiscal year. For additional information, please refer to the Commonwealth Universal Research Enhancement Annual C.U.R.E. Reports on the Department's Tobacco Settlement/Act 77 web page at <http://www.health.state.pa.us/cure>.

Research Project 11: Project Title and Purpose

Hyperhomocysteinemia and Thrombosis Formation - The purpose of this project is to identify the mechanistic links between HHcy and thrombosis in homocysteinemia animal model.

Duration of Project:

9/16/2008 – 5/10/2009

Summary of Research Completed

This project ended during a prior state fiscal year. For additional information, please refer to the Commonwealth Universal Research Enhancement Annual C.U.R.E. Reports on the Department's Tobacco Settlement/Act 77 web page at <http://www.health.state.pa.us/cure>.

Research Project 12: Project Title and Purpose

Identification of the Cis- and Trans- Elements Required for Stress-Mediated Induction of Gadd45B - Gadd45B is a small nuclear protein which is implicated in modulating the cellular response to physiological stresses. Gadd45B mRNA levels are robustly induced in mammalian cells following treatment with a variety of different stress agents, which either directly or indirectly damage DNA. The mechanism of this induction is unknown. Therefore, we plan to determine the extent to which this induction is regulated transcriptionally and post-transcriptionally, and identify cis elements and corresponding transcription factors required for induction. Knowledge of this mechanism is important in understanding how Gadd45B can become deregulated, and thus lead to a greater propensity to tumor growth and cancer.

Duration of Project

9/16/2008 – 6/30/2009

Summary of Research Completed

This project ended during a prior state fiscal year. For additional information, please refer to the Commonwealth Universal Research Enhancement Annual C.U.R.E. Reports on the Department's Tobacco Settlement/Act 77 web page at <http://www.health.state.pa.us/cure>.

Research Project 13: Project Title and Purpose

A Novel Approach for Engineering Neovasculature for Stem Cell Therapy - Most current pharmacological and/or invasive therapies aim to treat heart disease. During the past few years, however, there has been much excitement and interest in developing regenerative approaches for curing heart disease. Research is aimed at restoring the contractile function of the heart through engineering replacement myocardium and its supporting microenvironment using approaches such as cell-based therapy. Recent attempts at rebuilding the myocardium using stem cells have yielded disappointing results. The overall goal of this study is to develop the technology to enhance the morphology and function of post-infarct neovasculature, prior to scar formation, and to establish the optimal time post-myocardial infarction (MI) when proangiogenic interventional strategies could result in maximal in situ renewal of myocardial tissue which has been lost to MI.

Anticipated Duration of Project

1/30/2009 – 6/30/2011

Project Overview

The overall goal of this study is to develop the technology to enhance the morphology and function of post-infarct neovasculature, prior to scar formation, and to establish the optimal time post-myocardial infarction (MI) when proangiogenic interventional strategies could result in maximal in situ renewal of myocardial tissue. The specific aims of this study are to: 1) Develop immunoliposomes containing pro-angiogenic compounds (vascular endothelial growth factor (VEGF) and/or basic fibroblast growth factor (bFGF)) and determine their biodistribution in MI animals; 2) Selectively deliver pro-angiogenic compounds to the infarct region by targeting MI upregulated adhesion molecules in microvessels bordering on the infarct site, and quantify improvements in vascularity, perfusion, and cardiac function; and study the efficacy of combining stem cell therapy with targeted pro-angiogenic therapy to determine if this combinational therapy can significantly improve vascularity, perfusion, and cardiac function as compared to stem cell therapy alone.

In Specific Aim 1, we will use clinically relevant drug carriers (immunoliposomes) bearing mAbs to adhesion molecules that are upregulated on the vasculature of infarct tissue to show that particles can be targeted to infarct tissue and to optimize particle design and drug loading & release profiles in vitro. We will quantify the level and time course of the upregulation of E- and P-selectin, ICAM-1, and $\alpha\beta 3$ that are known to be upregulated in MI tissue to determine the best molecular target(s) and time point(s). In Specific Aim 2, functional significance of pro-angiogenic therapy will be assessed in terms of neovascular formation, oxygen delivery capacity, and cardiac function. Combinatorial effects of no treatment, targeted pro-angiogenic therapy, and

systemic pro-angiogenic therapy will be investigated. To bypass the potential side effects of systemic administration of proangiogenic compounds, we will use clinically relevant drug carriers (immunoliposomes) to deliver VEGF and/or bFGF to the infarct region via upregulated adhesion molecules. We will also investigate the enhancing effects of targeted pro-angiogenic therapy on marrow stromal cell treatment of myocardial infarction. A combinatorial design will be used to study the effects of stem cell therapy, targeted pro-angiogenic therapy, and systemic pro-angiogenic therapy on neovascular formation, generation of cardiomyocytes, and cardiac function. These findings will then be used to quantify the beneficial effects of combinational stem cell + targeted pro-angiogenic therapy to determine if targeted pro-angiogenic therapy can augment stem cell treatment. Infusion of these cells into the tail vein will approximate the clinical scenario of autologous intravenous cell therapy

Principal Investigator

Mohammad F. Kiani, PhD
Professor and Chair
Department of Mechanical Engineering
Temple University
1947 N. 12th St.
Philadelphia, PA 19122

Other Participating Researchers

Barbara Krynska, PhD, Linda Knight, PhD, Deborah Crabbe, MD, Ausim Azizi, MD, PhD - employed by Temple University

Expected Research Outcomes and Benefits

Myocardial infarction often leads to congestive heart failure and is a leading cause of death in the U.S. and other industrialized countries. In addition to the lost muscle mass, a transmural MI also involves the deterioration of the microenvironment through the proteolysis of extracellular matrix, vasculature, and nerves. Subsequent tissue repair usually does not involve a significant regeneration of the microenvironment and the microvasculature. Bold innovative strategies are needed to prevent the appearance of chronic cardiac failure following MI. Engineering replacement myocardium and its supporting vasculature, in approaches such as bone marrow-derived stromal cell (MSC) therapy or muscle cell transplantation, may represent such initiatives. Recent attempts at rebuilding the myocardium using stem cells have yielded disappointing results. The lack of a supporting vasculature which provides oxygen and nutrients for the differentiating stem cells may in part explain these disappointing findings. However, concerns over possible side effects have hampered attempts at revascularizing the infarcted myocardium using systemic delivery of pro-angiogenic compounds such as VEGF and bFGF. Recently, we have developed a novel approach for preferentially delivering drug-carrying immunoliposomes to infarct tissue by targeting cell adhesion molecules which are upregulated in the vasculature of infarcted myocardium. We seek to develop a novel methodology to enhance the morphology and function of infarct neovasculature, prior to scar formation, and to establish the optimal time post-MI when interventional strategies, e.g. MSC therapy, could result in maximal, in situ renewal of

myocardial tissue lost to MI. Our preliminary findings indicate that local delivery of pro-angiogenic compounds to the infarct region could initiate the regrowth of neovasculature supporting regeneration of myocardial tissue from stem cells, which in turn could lead to improved cardiac function. The long-term goal of this project is to develop a combined pro-angiogenic/stem cell therapy for restoring myocardial function in a clinical setting.

Summary of Research Completed

To study the effects of antibody conjugated drug carriers containing vascular endothelial growth factor (VEGF) on cardiac function and vascular density after an MI, we utilized echocardiography and histochemical staining techniques to quantify cardiac output and vascularization of the MI border zone, respectively. In this study, myocardial infarction was induced in male Sprague-Dawley rats through ligation of the left descending coronary artery. One minute after surgery, the treatment group (n = 10) received an injection of VEGF encapsulated immunoliposomes (0.12 µg/kg BW). Serial echocardiograms were performed the first three days, and then weekly, up to four weeks post-infarction, to characterize changes in left ventricular geometry and function over time. A sham (no MI) group (n = 5) and an untreated MI group (n = 7) were followed for comparison. After the fourth week, hearts were excised and stained for perfused and anatomical vessels. It was found that hearts treated with targeted VEGF showed a significant improvement in cardiac size, function, and vascular density, compared to untreated MI hearts.

Preparation of Stealth Immunoliposomes Containing VEGF

Pegylated lipids were used in the formulation of liposomes to decrease the uptake of the drug carriers in the liver and spleen. A maleimide group on the pegylated lipids was used to attach a thiolated antibody. Liposomes were composed of 50 mole % hydrogenated soy L- α -phosphatidylcholine (HSPC), 45 mole % cholesterol, 3 mole % 1,2-distearoyl-*sn*-glycero-3-phosphoethanolamine-N-[(polyethylene glycol)2000] (DSPE-PEG2000) and 2 mole % DSPE-PEG-maleimide (Avanti, Alabaster, AL). Lipids were dried under vacuum overnight (< 0.2 Torr), and then rehydrated in 37 °C deionized water and extruded (Lipex, Vancouver, BC, Canada) 10 times with a 0.2 micron filter (Nucleopore), yielding a liposome diameter of 180.0 ± 13 nm.

IgG_{2a} mAb RMP-1 to rat P-selectin was thiolated in an iminothiolane buffer, then conjugated to the immunoliposomes by incubating the thiolated antibody with the liposomes overnight at 4 °C. The unconjugated antibody was separated from the liposomes by ultracentrifugation, then the immunoliposomes were freeze-dried under vacuum overnight with 100µg of human VEGF_{165A} (Genentech Inc, San Francisco, CA). The following day, immunoliposomes were rehydrated in a Tris buffer (pH 7.4) solution at 37°C and gently vortexed until vesicles were fully reformed and then incubated at room temperature for 1 hour. Free VEGF (not encapsulated) was separated from the immunoliposomes with a Hi Trap Heparin HP Column (GE Healthcare, Piscataway, NJ). Immunoliposomes were then resuspended in Tris buffer to a working 10mM lipid concentration.

Rat Infarction Model

All animal procedures were performed in accordance with protocols approved by The Institutional Animal Care and Use Committee (IACUC). Six-week old male Sprague-Dawley rats (150-160 grams) were obtained from Harlan Laboratories (Indianapolis, Indiana) for these studies. All rats were housed 2 animals per cage, received 12 hour light/dark cycle and were fed standard rat chow. Anesthesia was induced using Isoflurane (4% induction, 2% maintenance) and the animals received ventilatory support. Upon adequate anesthesia, a left thoracotomy and pericardiotomy were performed, the heart was rapidly exteriorized, and ligation of the left anterior descending coronary artery was performed using a 6.0 silk suture. Upon completion of the procedure, the chest was closed and the lungs re-inflated using positive end-expiratory pressure. The animals were allowed to recover at ambient room temperature and were available for additional studies twenty-four hours after surgery. The presence of an MI was verified using echocardiography 24 hours after surgery based on elevation or depression of ST segment or T wave inversion, and ceased motion of the anterior left ventricular wall.

Treatment Protocol

For geometrical and functional ECHO studies, animals that underwent MI surgery were randomly assigned to one of five groups: anti-P-selectin conjugated immunoliposomes containing VEGF (0.12 ug/kg BW, n = 10), empty anti-P-selectin conjugated immunoliposomes (n = 5), non-specific binding immunoliposomes containing VEGF (0.12 ug/kg BW, n = 4), systemic VEGF (30 ug/kg BW, n = 3), or no treatment (n = 7). Animals with no MI were matched by body weight and followed for comparison (n = 5). Animals treated with targeted VEGF at 4 hours (n = 4) and 24 hours (n = 4) post-infarction were followed to determine the effects on injection time. For vascular studies, animals were assigned to one of the following groups: anti-P-selectin conjugated immunoliposomes containing VEGF (0.12 ug/kg BW, n = 7), no treatment (n = 5).

Transthoracic Echocardiography

Transthoracic echocardiograms were performed after semi-conscious sedation was administered intramuscularly using Xylazine (10 mg/kg) and Ketamine (50 mg/kg). After anesthesia, each animal had their chests shaved and was placed in the supine position for imaging. Imaging began 5 minutes after the administration of sedation to allow the heart rate to stabilize. A Philips Sonos 5500 machine and a multi-frequency transducer set at 12 MHz was used for 2-D imaging. Imaging was performed using a depth of 2 cm. Echocardiograms analyzed by different operators were shown to be highly reproducible using an intraclass correlation, obtained using a two-way mixed effect model, to assess consistency of measurements.

Regional wall motion assessment was used to give a non-invasive evaluation of left ventricular function and internal chamber dimensions. The left ventricular end-diastolic (LVEDD) and end-systolic (LVESD) diameters were measured, along with anterior and posterior wall thickness. All measurements were made using the leading-edge method. Fractional shortening and ejection fraction were calculated using equations 1.2 and 1.3. A large MI was defined as a significant increase in the LVEDD greater than two standard deviations above the normal chamber size.

Quantify Changes in Vascularity Through Histochemical Staining

Previously, immunohistochemical and histochemical staining techniques were developed to quantify the density of perfused and anatomical vessels in the border zone of an MI. Briefly, DiOC₇ was injected via tail vein into an unconscious animal, and one minute later the heart was excised and frozen. Sections were taken at 9 μm through the infarct region, and images were viewed using fluorescent microscopy (490 nm excitation, 520 nm emission) on a Nikon Eclipse TE200. Images were acquired for analysis using a monochrome Q Imaging Retiga 1300 camera and ImagePro imaging software. These images were used to determine the average distance of tissue to the nearest perfused vessel. The distribution of distances from the nearest vessel can be used as an index of effective oxygen diffusion distance in tissue to assess adequacy of microvascular flow. Anatomical vessels were stained using CD31 (BD Biosciences, Franklin Lakes, NJ), then imaged using the monochrome Q Imaging Retiga 1300 camera and a Nikon Eclipse TE200.

Statistical Analysis

Results are expressed as the mean value ± SEM. The significance of differences between three experimental groups was determined by one-way Analysis of Variance (ANOVA, SigmaStat 3.1, Systat Software Inc., San Jose, CA). The Kolmogorov-Smirnov Test (using Statgraphics Centurion XV, StatPoint Inc., Herndon, VA) was used to determine significant differences in the distribution of distances to the nearest perfused vessel. Values of $p < 0.05$ were considered statistically significant.

Results

Serial echocardiograms characterized adverse geometrical and functional changes in hearts of all MI groups, compared to sham hearts with no MI. Interior dimensions of the left ventricle in both diastole and systole were greater in MI hearts than sham hearts four weeks after the induction of MI (Figure 1). Hearts treated with targeted VEGF therapy exhibited less dilation in both diastole and systole at four weeks post-infarction, compared to untreated MIs and compared to systemic VEGF, empty targeted immunoliposome, and non-targeted VEGF immunoliposome treated (data not shown).

Likewise, hearts treated with targeted VEGF therapy showed significant increases in fractional shortening and ejection fraction, compared to untreated MIs and other control MI groups (data not shown), suggesting improvements in overall stroke volume of the left ventricle (Figure 2).

Animals treated with targeted VEGF therapy at 4 hours and 24 hours post-infarction exhibited a similar trend in fraction shortening over a period of four weeks after induction of infarction, compared to the experimental group that received treatment immediately following the induction of an MI (Figure 3).

Hearts treated with targeted VEGF therapy also experienced an increase in vascular density of both perfused and anatomical vessels in the border zone of the MI, compared to untreated MIs. Figure 4 qualitatively shows normal healthy vascular density compared to a severely decreased vascular density after an MI. MIs treated with targeted VEGF therapy exhibit greater vessel density for both perfused and anatomical vessels, compared to untreated MIs.

The cumulative frequency of distance to the nearest perfused vessel (Figure 5) serves as an index of oxygen diffusion to the surrounding tissue. Targeted VEGF therapy resulted in improvements (i.e., decreases) in the distance to the nearest perfused vessel as compared to untreated MI animals. These improvements in the perfusion distance are associated with improvements in cardiac geometry and function.

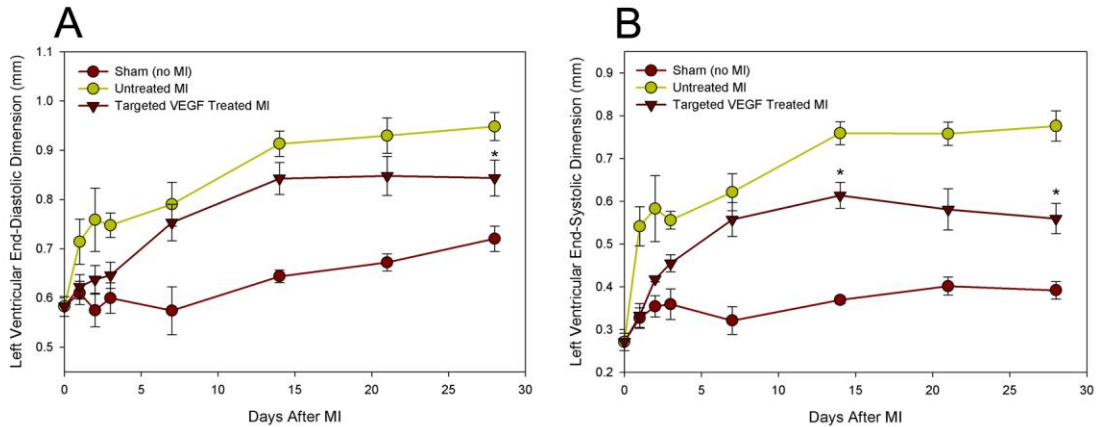


Figure 1. Left ventricular dimensions during A.) diastole, and B.) systole for sham (no MI), targeted VEGF treated MIs, and untreated MIs. Targeted VEGF therapy resulted in a significant decrease in left ventricle dilation at four weeks post-infarction, compared to the untreated MI group.

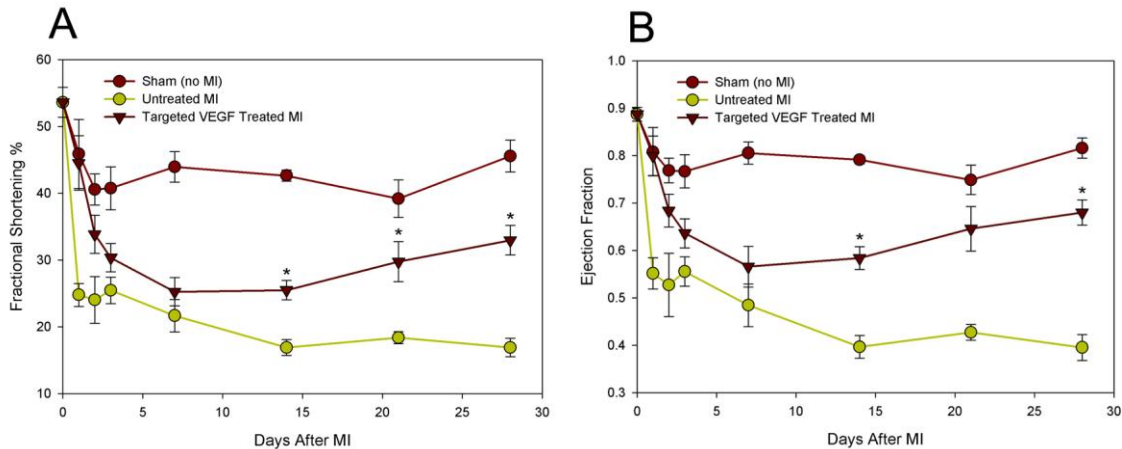


Figure 2. Functional changes measured as A.) Fractional shortening, and B.) ejection fraction, for sham (no MI), targeted VEGF treated MIs, and untreated MIs. Hearts treated with targeted VEGF therapy showed significant increases in both fractional shortening and ejection fraction up to four weeks post-infarction, compared to the untreated MI group.

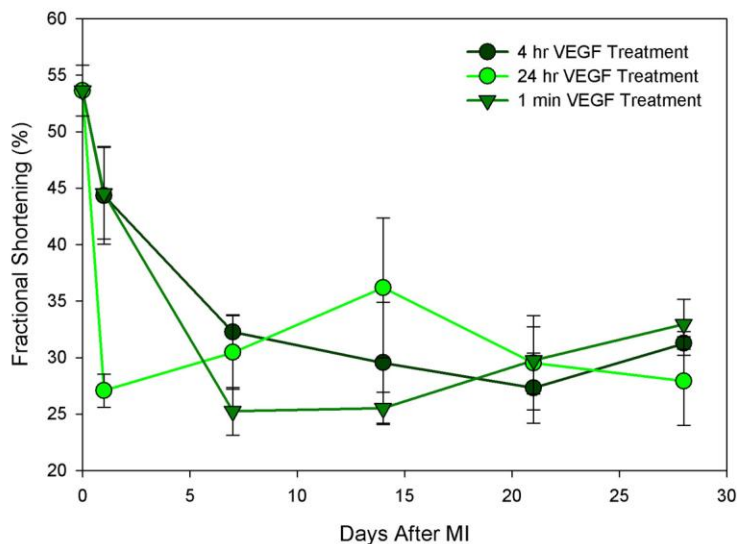


Figure 3. Animals treated with targeted VEGF therapy 4 hours and 24 hours exhibited no significant difference in fractional shortening compared to animals treated with targeted VEGF therapy immediately following the induction of MI.

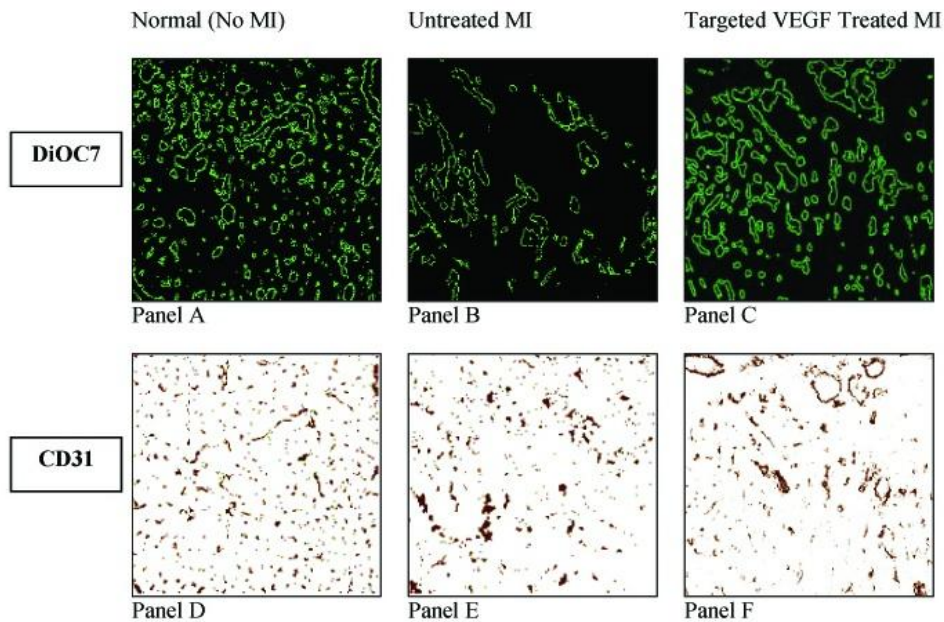


Figure 4. Panels A, B, and C: DiOC₇ stains for perfused vessels for sham (no MI), untreated MI and targeted VEGF treated MI, respectively. Panels D, E, and F: CD31 was used to stain for anatomical vessels for sham (no MI), untreated MI and targeted VEGF treated MI, respectively. Both MI groups show a decrease in vascular density at four weeks post-infarction, but hearts treated with targeted VEGF showed a significantly greater vascular density than untreated MI hearts.

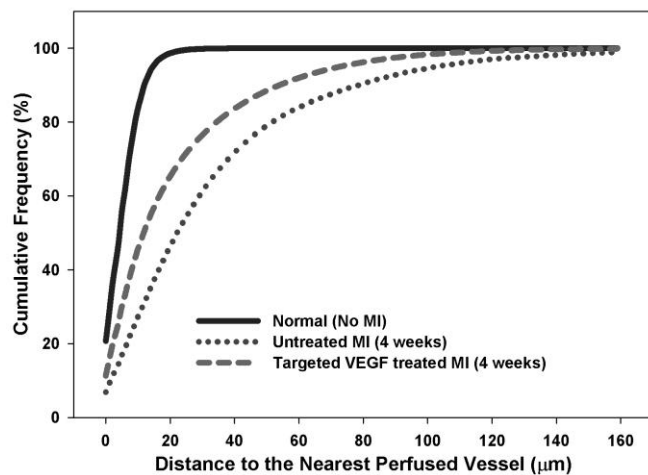


Figure 5. The cumulative frequency of myocardial tissue distance to the nearest perfused vessel was quantified at four weeks post-infarction. Healthy tissue is within 20 microns distance to a perfused vessel. Following an MI, vessel density in the border zone of the MI decreases significantly, but hearts treated with targeted VEGF therapy have a greater percentage of tissue within 20 microns of a perfused vessel compared to untreated MI hearts.

Research Project 14: Project Title and Purpose

Omega-3 Fatty Acids as Therapeutic Anti-inflammatory Agents - In recent years inflammation has emerged as an essential underlying process in diseases of various etiologies such as Alzheimer's disease, cardiovascular diseases and cancer, which joined classical inflammatory/autoimmune disorders such as arthritis, periodontal disease, septic shock, inflammatory bowel diseases, multiple sclerosis, lupus erythematosus, etc. Although both steroidal and nonsteroidal anti-inflammatory therapies have been developed, there is a pressing need for new therapeutic anti-inflammatory agents with fewer side effects and better efficacy.

Anticipated Duration of Project

1/30/2009 – 6/30/2011

Project Overview

Omega-6 and omega-3 fatty acids obtained solely from food are essential for human health. Omega-6 fatty acids are abundant in land animals, whereas omega-3 fatty acids are preponderant in marine mammals and fatty fish. Preponderance of fish in the diet is associated with reduced incidence of inflammatory and cardiovascular diseases, and dietary supplements containing mixtures of the major omega-3 fatty acids eicosapentaenoic acid (EPA) and docosahexaenoic acid (DHA) have a beneficial effect in several human inflammatory conditions.

In the present project we will investigate the effects of the omega-3 fatty acid DHA in models of inflammatory bowel disease (IBD). Human IBD are chronic, relapsing disorders, characterized by inflammatory reactions to microbial antigens. Despite recent advances in research and therapeutic approaches, IBD patients are often resistant to treatment, justifying the search for new therapies. Murine IBD models have been used extensively for mechanistic studies and proof of concept in therapeutic interventions. We propose to use the TNBS colitis model, a model for human Crohn's disease, to assess the anti-inflammatory effects of DHA and to investigate some of the molecular mechanisms involved in the therapeutic effect.

1. *DHA effects on disease.* We will assess DHA effects on disease prevention, on established disease and on disease recurrence. We expect that DHA will have a protective effect, by reversing established disease and preventing recurrence.
2. *Effects of DHA on colonic cellular composition and function.* The protective effects might be due to reduced infiltration of inflammatory cells. Colons will be examined for macroscopic and histology scores, myeloperoxidase activity (reflective of neutrophil infiltration), and T cell, monocyte/macrophages, and dendritic cell infiltration. Colonic expression of proinflammatory cytokines and chemokines will be determined.
3. *Effects of DHA on T cell differentiation.* DHA might affect T cell differentiation. If this is the case, we will observe changes in the numbers of IFN γ +, IL-4+, IL-17+ T cells. Mesenteric lymph node cells will be analyzed in terms of T cell proliferation and for intracellular and/or secreted cytokines characteristic for the effector T cell subsets Th1, Th2, Th17 and Treg.

Principal Investigator

Doina Ganea, PhD
Professor and Chair
Department of Microbiology & Immunology
Temple University
3400 N. Broad St.
Philadelphia, PA 19140

Other Participating Researchers

Jui-Hung Yen, PhD – employed by Temple University

Expected Research Outcomes and Benefits

The project will provide information on the anti-inflammatory role of omega-3 fatty acids in experimental models of inflammatory bowel diseases, and will contribute to the understanding of the cellular/molecular mechanisms involved in the protective and/or therapeutic effects of omega-3 fatty acids. These results will provide supporting evidence for future clinical trials using omega-3 fatty acids and their derivatives in gastrointestinal disorders of an inflammatory nature. Since patients suffering from such disorders are often resistant to existing therapies, this project could have a significant impact on the improvement of human health.

Summary of Research Completed

In the previous period of support we tested the preventive effects of docosahexaenoic acid (DHA) in TNBS-induced colitis. As previously reported, i.p. DHA administration had a significant protective effect. We extended the previous experiments by performing histological and molecular analyses. Colons were examined on day 4 for macroscopic evaluation and histology scores. As expected, the DHA treatment resulted in reduced histology scores, reduced numbers of infiltrating inflammatory cells, reduced neutrophil infiltration (measured by myeloperoxidase activity), reduced levels of proinflammatory cytokines and increased levels of the anti-inflammatory cytokine IL-10 in the peritoneal fluid. In terms of effects of T cell differentiation we analyzed mesenteric lymph node cells for production of IFN γ (Th1), IL-17 (Th17), IL-4 (Th2) (Fig.1). DHA treatment reduced the levels of IFN γ and IL-17 (Fig.2), which indicates that the differentiation of the proinflammatory subsets Th1 and Th17 has been inhibited by DHA. IL-4 was below detection levels. We next investigated whether DHA treatment would be effective during fully established colitis. Mice were treated with lower doses of TNBS (1.5 mg/ml) and DHA was administered on three consecutive days starting six days after disease onset. We did not observe any effect on the disease outcome. We also examined whether DHA was able to prevent disease recurrence. Mice that received TNBS (3 mg/ml) and were treated with DHA on day 0 and +1, were re-exposed to TNBS on day 9. Contrary to our expectations, the DHA treatment did not protect mice from disease recurrence, whereas controls receiving cortistatin survived and did not exhibit clinical symptoms. This does not preclude a possible effect in established disease or on disease recurrence upon use of dietary DHA, especially since omega 3 fatty acids require prior incorporation in cell membranes. Such experiments are now in progress with funding from a different source.

Analysis of cellular infiltrates in the peritoneal exudate indicated reduced numbers of neutrophils and T cells in mice treated with DHA as compared to TNBS controls. However, to our surprise the numbers of dendritic cells, known activators of T cells in DHA treated mice were not reduced and in some cases even increased. To explain this apparently contradictory result, we initiated a series of in vitro experiments looking at the effects of DHA on dendritic cell (DC) phenotype and function. These studies resulted in a manuscript that has been published in [Lipids Health Dis.](#) 2010 Feb 1;9:12 entitled "Docosahexaenoic acid prevents dendritic cell maturation and in vitro and in vivo expression of the IL-12 cytokine family" by [Kong W](#), [Yen JH](#), [Vassiliou E](#), [Adhikary S](#), [Toscano MG](#), [Ganea D](#). PMID: 20122166. The results are summarized in the Abstract below:

Abstract

BACKGROUND: Acute and chronic inflammation play essential roles in inflammatory/autoimmune conditions. Protective anti-inflammatory effects of the n-3 fatty acids docosahexaenoic acid (DHA) and eicosapentaenoic acid (EPA) were reported in animal models of colitis, sepsis, and stroke. Since dendritic cells (DC) represent the essential cellular link between innate and adaptive immunity and have a prominent role in tolerance for self-antigens, we sought to investigate the impact of DHA on DC maturation and proinflammatory cytokine production. **METHODS:** Murine bone marrow-derived DC were treated with DHA and stimulated with various toll-like receptor (TLR) ligands. Flow cytometry was used to determine the levels of surface maturation markers and endocytic activity. Cytokine expression and

secretion were measured by real-time RT-PCR and ELISA assays. PPARgamma and NFkappaB activity in nuclear extracts were determined by binding to specific oligonucleotide sequences using ELISA-based assays. In vivo effects of DHA were assessed in splenic DC from LPS-inoculated mice maintained on a DHA-enriched diet. RESULTS: DHA maintained the immature phenotype in bone marrow-derived DC by preventing the upregulation of MHCII and costimulatory molecules (CD40, CD80 and CD86) and maintaining high levels of endocytic activity. DHA inhibited the production of pro-inflammatory cytokines, including the IL-12 cytokine family (IL-12p70, IL-23, and IL-27), from DC stimulated with TLR2, 3, 4, and 9 ligands. DHA inhibition of IL-12 expression was mediated through activation of PPARgamma and inhibition of NFkappaBp65 nuclear translocation. DHA exerted a similar inhibitory effect on IL-12 and IL-23 expression in vivo in LPS-inoculated mice maintained on a DHA-enriched diet. CONCLUSIONS: Exposure of bone marrow-derived DC to DHA resulted in the maintenance of an immature phenotype and drastic reduction in proinflammatory cytokine release. DHA inhibited the expression and secretion of the IL-12 cytokine family members (IL-12p70, IL-23 and IL-27), which play essential roles in the differentiation of the proinflammatory Th1/Th17 effector cells. The effect of DHA on IL-12 expression was mediated through activation of PPARgamma and inhibition of NFkappaB. Inhibition of IL-12 and IL-23 expression was also evident in splenic DC from mice fed a DHA-enriched diet, suggesting that dietary DHA acts as an anti-inflammatory agent in vivo.

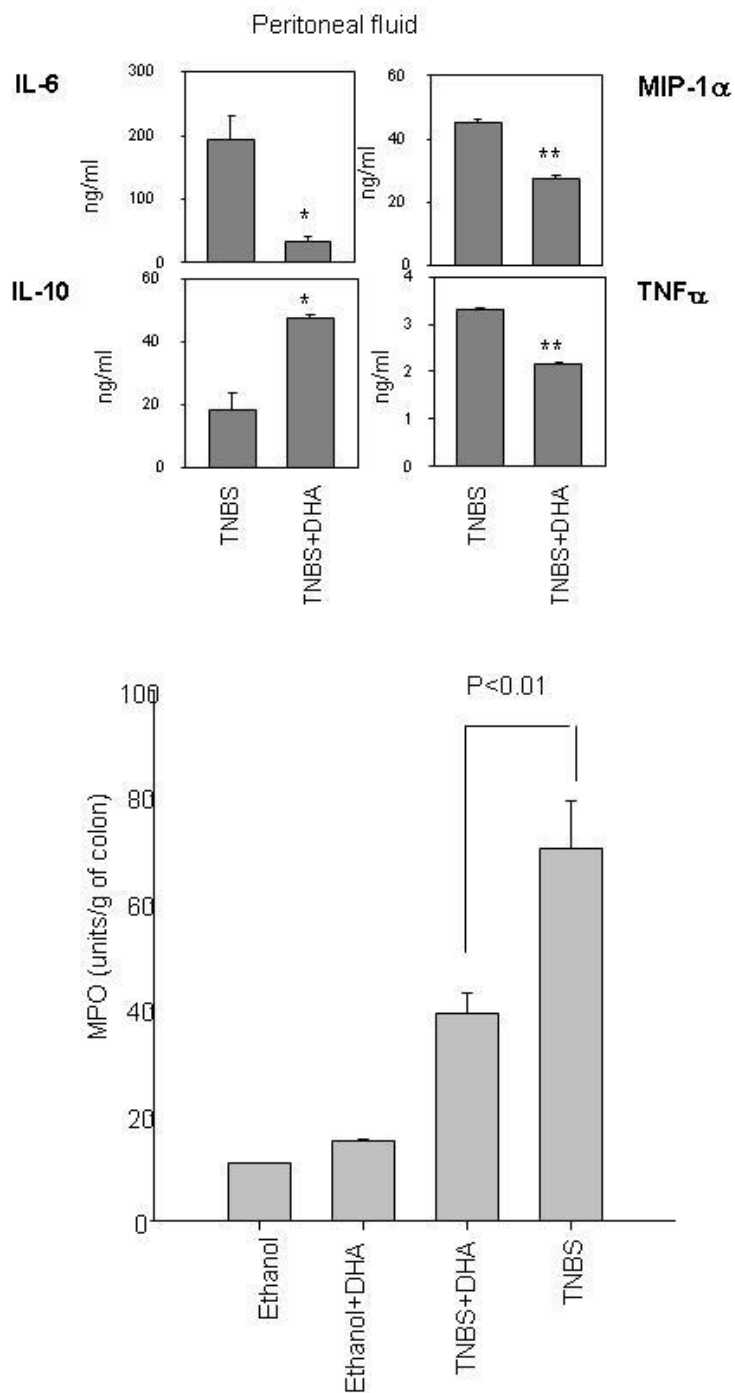


Figure 1 Peritoneal fluid from day 4 was analyzed for cytokine production. Colons on day 4 were homogenized and analyzed for MPO (myeloperoxidase) activity.

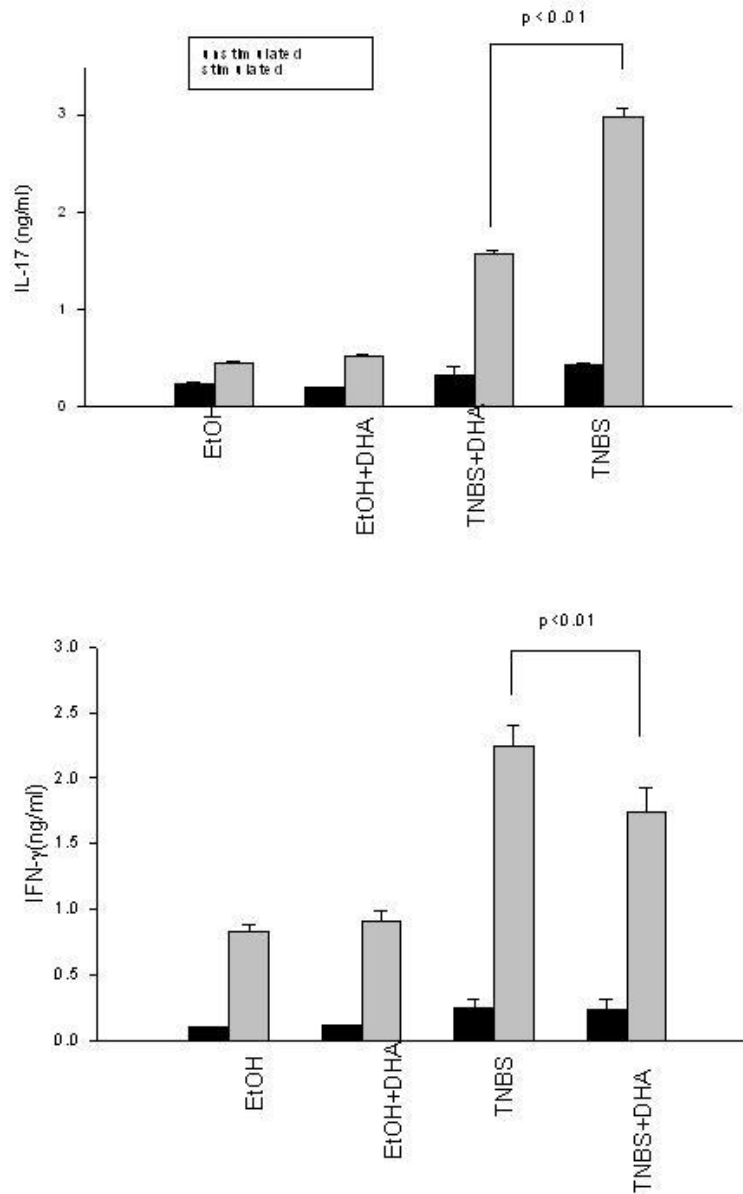


Figure 2

Mesenteric lymph node cells were restimulated with PMA and ionomycin and analyzed for IL-17 (Th17), IFN γ (Th1) and IL4 (Th2) cytokine production. IL-4 levels were undetectable.

Research Project 15: Project Title and Purpose

Angiocidin Induces Stem Cell Activation and Differentiation - Our laboratory has discovered a protein which we call angiocidin. When the protein is injected into mice that have cancer, it keeps the cancer from growing and spreading. The purpose of our project is to see if angiocidin inhibits cancer growth by inhibiting the growth and spread of cancer stem cells, a subset of cancer cells that are thought to cause cancer growth and spread.

Anticipated Duration of Project

1/30/2009 – 12/31/2010

Project Overview

We hypothesize that angiocidin differentiates THP-1 leukemia cells as well as other tumor cells into a more normal phenotype by activating and differentiating stem cells present in the tumor cell population to a more normal phenotype that is not tumorigenic. We base our hypothesis on the observation that angiocidin-treated THP-1 cells up-regulated CEA-CAM-1, a major stem cell marker, discovered by comparing the microarray profiles of cells treated with angiocidin with that of controls. Additionally, in a collaboration with Dr. John Wong, CEO of Moraga Biotech Corporation (<http://www.moragabiotech.com>), we observed that angiocidin activated and differentiated normal blood stem cells into a fibroblast-like phenotype when cultured on collagen. These cells not only expressed CEA-CAM-1 but were also stimulated to proliferate in response to angiocidin - an effect that was more potent than that obtained with growth factors such as basic fibroblast growth factor. Temple University is filing a provisional patent application seeking patent protection for the observation that angiocidin can activate and stimulate stem cell differentiation. The benefits of this research relate not only to angiocidin-mediated cancer treatment but also to angiocidin-mediated stimulation of tissue regeneration and wound healing.

Based on these observations, we propose to test directly our hypothesis that angiocidin can activate cancer stem cells and differentiate them into a more normal phenotype. We have obtained a human melanoma stem cell line from Dr. Meenhard Heryln of the Wistar Institute. These cells are highly tumorigenic but can be differentiated into normal melanocytes. In this project, we propose to culture these cells in the presence and absence of angiocidin. We will compare the gene expression profiles of control and angiocidin-treated cells using microarray analysis and PCR arrays. We anticipate that the angiocidin-treated cells will up-regulate melanocyte markers and down-regulate markers characteristic of melanoma. The in vitro functional activity of control and angiocidin-treated cells will also be evaluated in proliferation, adhesion and migration assays. The in vivo tumorigenic activity of control and angiocidin-treated cells will be evaluated in athymic mice injected subcutaneously with either control or angiocidin-treated cells. We anticipate that the angiocidin-treated cells will lose their ability to form tumors. The results of these studies will provide proof-of-concept that angiocidin activates and differentiates cancer stem cells making them less tumorigenic.

Principal Investigator

George Tuszynski, PhD
Professor
Temple University
1900 North 12th Street
Philadelphia, PA 19122

Other Participating Researchers

Vicki Rothman, BS – employed by Temple University

Expected Research Outcomes and Benefits

We hope to show that angiocidin, a protein that our laboratory discovered and has been studying for its anti-cancer activity, has a direct inhibitory effect on the ability of cancer stem cells to grow and spread as tumors. We will evaluate the effect of angiocidin on melanoma stem cells but also other cancer stem cells isolated from human cancers. We will analyze the gene composition of cancer stem cells treated with angiocidin and hope to show that angiocidin causes cancer stem cells to express fewer cancer genes and more normal genes. Our studies should directly benefit cancer patients by providing them a cancer therapy that targets cancer stem cells. The potential advantage of this type of therapy is that once patients are treated with stem cell targeting agents such as angiocidin, the cancer is less likely to come back since cancer stem cells are thought to be responsible for the recurrence of cancer. There is currently no cancer therapeutic that effectively targets cancer stem cells.

Summary of Research Completed

In the current grant period we have obtained the following results: We found that angiocidin promoted PC-12 neurite outgrowth. In the next section the data is presented with detailed experimental procedures.

Angiocidin promotes PC12 neurite outgrowth

PC12 is a cell line derived from a pheochromocytoma of the rat adrenal medulla (*Greene LA, Tischler AS (July 1976). "Establishment of a noradrenergic clonal line of rat adrenal pheochromocytoma cells which respond to nerve growth factor". Proc. Natl. Acad. Sci. U.S.A. 73 (7): 2424–8.*). PC12 cells stop dividing and terminally differentiate when treated with nerve growth factor (NGF). These cells are a neuroblastoma cell line that originated from neurons. PC12 cells stop dividing and terminally differentiate when treated with nerve growth factor (NGF) as well as other factors belonging to the NGF family of neurotrophins. This makes PC12 cells an important model system to study neuronal differentiation and neurogenesis. We found that angiocidin significantly promoted NGF-promoted differentiation of PC12 cells. We found that angiocidin promotes NGF-promoted differentiation of PC12 cells.

Briefly, PC-12 Cells were plated in six well plates at a density of 2.5×10^5 cells/mL in 1 mL of Dulbecco's Modified Eagle Medium (DMEM) containing 1% horse serum and 1% Penicillin and streptomycin, treated with 100 ng/mL of NGF, 1ug/mL of recombinant angiocidin, or both and allowed to incubate at 37° for 72 hours. After 72 hours, pictures were taken of five random fields at 400X using Hoffman lens. Figure 1 shows how we measured the neurites in the micrographs. Quantitation of neurite density was performed using Image J length analysis. To be considered a neurite, a process had to meet the following criteria: 1. Neurite had to be at least 10 um in length. 2. Neurite had to start and end within the field of vision. 3. Neurites with branches were measured to the branching point and then each branch was measured separately as shown below.

We found that in the presence of 1 microgram/ml of angiocidin the maximum length of the neurites (Figure 2) and the number of neurites per cell (Figure 3) increased by 30% and 20%, respectively. We also found that angiocidin promotes longer neurites with length greater than 20 microns as compared to NGF (Figure 4). Figure 5 summarizes the effect of angiocidin on neurite outgrowth. We found that angiocidin only in the presence of NGF promoted neurite outgrowth suggesting that angiocidin promotes the activity of NGF.

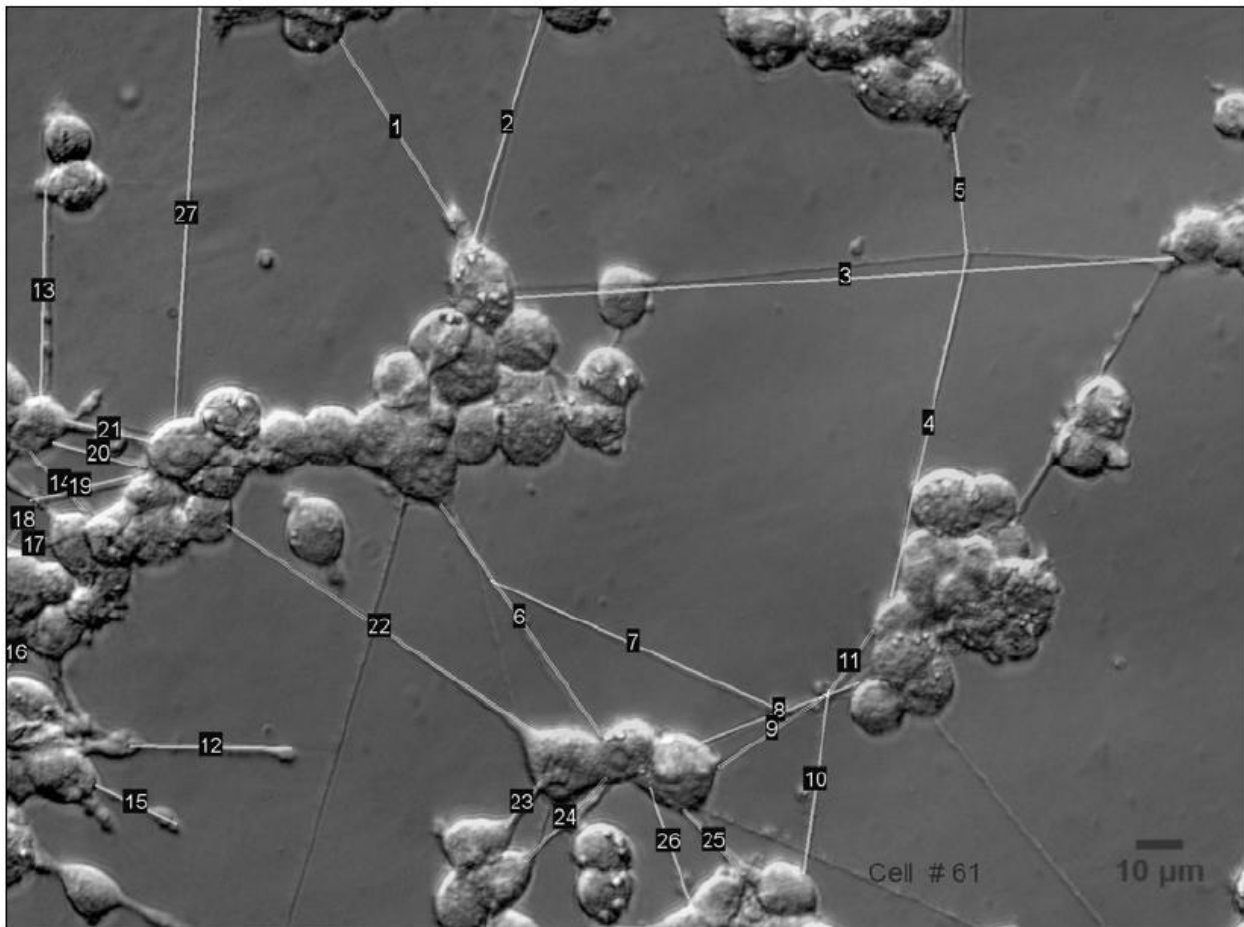


Figure 1: Example of neurite counting
(Ang. 1ug + NGF 100ng)

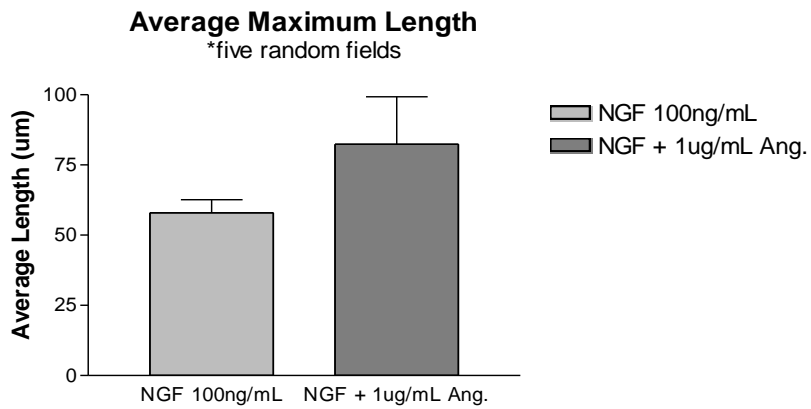


Figure 2 Average maximum length of neurites

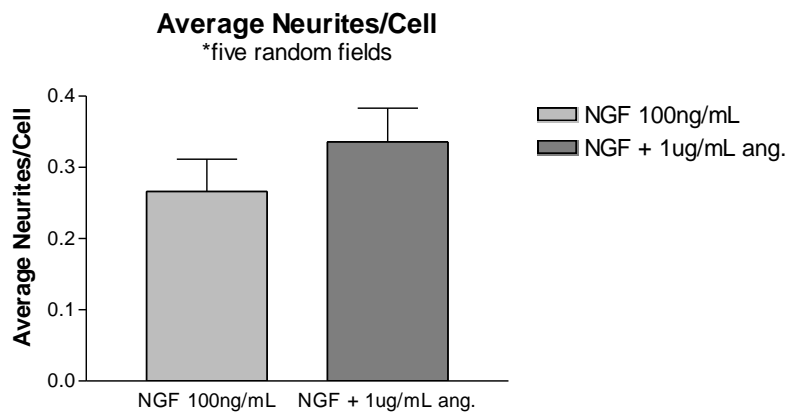


Figure 3 Average number of neurites per cell

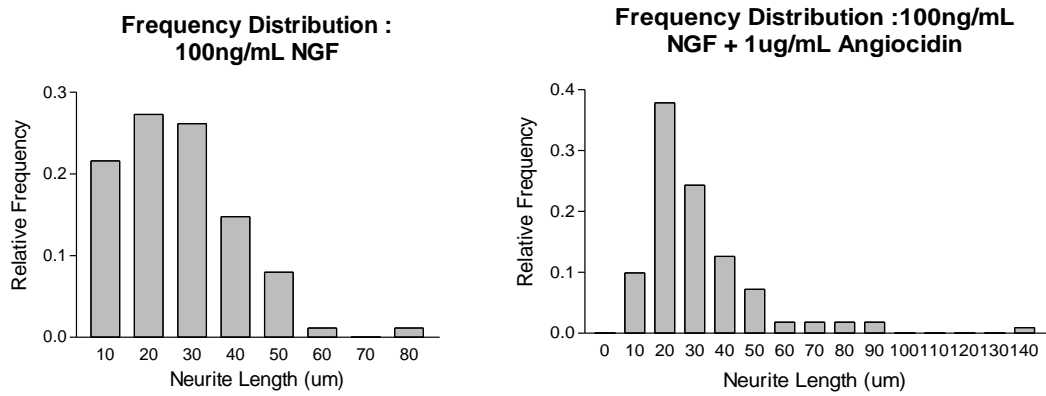


Figure 4 The effect of angioidin on the distribution of neurite length.

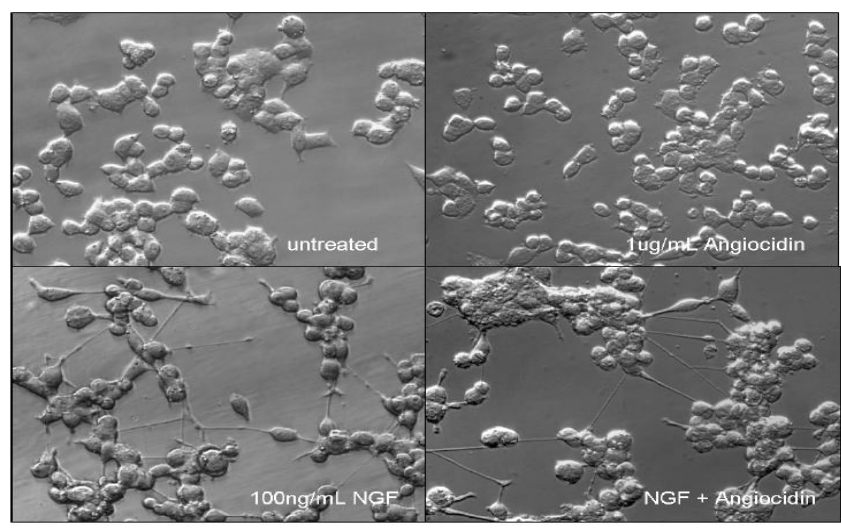


Figure 5 The effect of 1 microgram/ml of angioidin on PC-12 neurite outgrowth stimulated by 100 ng/ml of NGF. PC-12 cells were treated for 72 hours.

Research Project 16: Project Title and Purpose

Diversification of Streptococcus pyogenes during Persistence - The bacteria *Streptococcus pyogenes* causes many human diseases including pharyngitis (strep throat), impetigo (skin infection), streptococcal toxic shock syndrome and necrotizing fasciitis. In addition, after these acute diseases have been cured, post-streptococcal sequelae can develop that affect the heart (rheumatic fever) and kidneys (glomerulonephritis). To cause this myriad of diseases, *S. pyogenes* produces many virulence factors. When *S. pyogenes* is isolated from a patient, the strains are often not the same. This diversity of strains makes it difficult to determine which virulence factors are contributing to which diseases. The goal of this project is to determine, using laboratory models, how *S. pyogenes* diversify into unique strains during slow growth in stationary phase or inside human (eukaryotic) cells.

Duration of Project

1/30/2009 – 3/29/2010

Project Overview

Streptococcus pyogenes is a Gram-positive coccus that causes a wide range of diseases included acute infections such as pharyngitis, streptococcal toxic shock syndrome and necrotizing fasciitis. After acute infection, *S. pyogenes* can cause rheumatic fever and glomerulonephritis. Finally, *S. pyogenes* can be asymptotically carried by school-age children and adults. There is significant diversity of *S. pyogenes* strains making it difficult to associate virulence factors with disease progression and outcome. The mechanisms that drive this diversity are not understood. During studies on persistence in stationary phase batch culture and eukaryotic co-culture, we observed that the newly arisen strains of *S. pyogenes* had different stable exponential phase metabolisms and proteomes than the parental strain. One of three intracellular clinical isolates obtained from A. Podbielski (University of Rostock, Germany) expressed changes in exponential phase metabolism similar to the in vitro persisters. Taken together, these results led to the following model of *S. pyogenes* diversification. During pharyngitis *S. pyogenes* grows on tonsillar surfaces. A small percent of the *S. pyogenes* can invade epithelial cells. When the patient is treated with antibiotics such as penicillins that cannot penetrate the eukaryotic cell, the bacteria can persist within the eukaryotic cells. During persistence diversity is generated giving rise to unique strains of *S. pyogenes* that can reemerge after treatment is completed. These strains could give rise to recurrent tonsillitis, toxic shock syndrome, necrotizing fasciitis, and new epidemic strains. The first specific aim of this project is to determine if persister strains isolated from a single patient are diverse. Strains will be obtained from A. Podbielski (University of Rostock, Germany). Metabolic profiling and transcription of metabolic genes will be used to determine metabolic diversity. Real-time PCR will be used to assess differences in transcription of key virulence factors. The second specific aim of this project is to determine the basic mechanism(s) for the observed proteomic changes in the in vitro persisters. Persister strains generated from the parental stain CS101 will be compared to determine if diversity is occurring due to mutation or genomic rearrangement or both. The long-term goal of this research is to understand the mechanisms of diversity generation in *S. pyogenes*. If the generation of diversity can be blocked, it may significantly impact the emergence of new strains,

which can cause severe disease such as necrotizing fasciitis and streptococcal toxic shock syndrome, and significantly increase the efficacy of a *S. pyogenes* vaccine.

Principal Investigator

Bettina A Buttarò, PhD
Associate Professor
Department of Microbiology and Immunology
Temple University School of Medicine
3400 N. Broad St.
Philadelphia, PA 19140

Other Participating Researchers

Kathryn Weinstein – Graduate Student

Expected Research Outcomes and Benefits

Understanding how *S. pyogenes* diversifies will have two major impacts.

(1) The diversity of *Streptococcus pyogenes* strains is a major roadblock in the understanding how *S. pyogenes* causing diseases such as necrotizing fasciitis (flesh eating strep) because the strains isolated from different patients are different. It has been assumed that all the *S. pyogenes* causing a disease are the same in a single patient, so only one bacteria from the host is actually chosen to be studied in the laboratory. If we demonstrate a person may be colonized by more than one type of *S. pyogenes*, it would imply that more than one bacteria needs to be studied from a single patient when the person develops severe disease. This may change the approach to collecting disease isolates and allow for better correlation of virulence factor expression and disease outcome.

(2) The ability to diversify may be a key process in the ability of *S. pyogenes* to survive in the host and to cause a wide variety of diseases. The molecular pathways leading to diversification may be excellent targets for anti-microbial therapies that will inhibit both disease and the development of new strains.

Summary of Research Completed

Publications:

Wood*, D.N., Weinstein,* K. E., Podbielski, A., Kreikemeyer, B. Gaughan, J.P., Valentine, S., and Buttarò, B. A. Generation of metabolically diverse strains of *Streptococcus pyogenes* during persistence in stationary phase. *J. Bacteriol.* 191:6242-52, 2009.

Weinstein, K. E., Runft, D. L., Meissler, J., Eisenstein, T. K., Neely, M. N. and Buttarò, B. A. *S. pyogenes* survival gives rise to strains with changes in virulence, submitted, JID

Specific Aim 1 Determination of whether clinical isolates from a single patient are diverse. We are still in the process of obtaining funding to undertake the sequencing of strains and the construction of microarrays to determine genomic variability in isolates from a single patient. In the interim, we determined that survival in stationary phase and eukaryotic cells, gave rise to

strains with altered virulence properties. Stationary phase survivor strains (Alt. 1, Alt. 2, Alts. 4A and 4B) and intracellular survival strains (E11, E47.5-47.8) showed diversified expression of the virulence factors *emm*, *slo*, and *speB*, while expression of *prtF2* remained the same between the strains (Fig. 1 and Fig. 2). Zebrafish infection using these survivor strains revealed that all stationary phase survivor strains had attenuated virulence, and 2 of 5 intracellular survival derived strains had attenuated virulence (Table 2). Most of the attenuated survivor strains disseminated to the spleen but did not survive, and the strains were cleared by 3 days post-infection (Table 3). A whole blood killing assay using human blood from normal healthy donors showed a strong correlation between bacterial killing and *emm* expression (Fig. 3). The multilocus sequence type for the strains did not change (data not shown). Overall, these results suggest that during survival in the host, *S. pyogenes* can diversify into a phenotypically mixed population of cells that can still maintain their multilocus sequence type.

Specific Aim 2 Determine the basic mechanism(s) of the observed changes. To study the mechanism of allelic mutation, the putative error prone polymerase of *S. pyogenes* (*dinP*) has been mutated and its mutation rate is being compared to the parental strain during exponential growth and at different timepoints in stationary phase. To determine if changes in genetic content are occurring, differentially marked strains, are being compared for exchange of genetic markers during survival in mixed cultures in stationary phase.

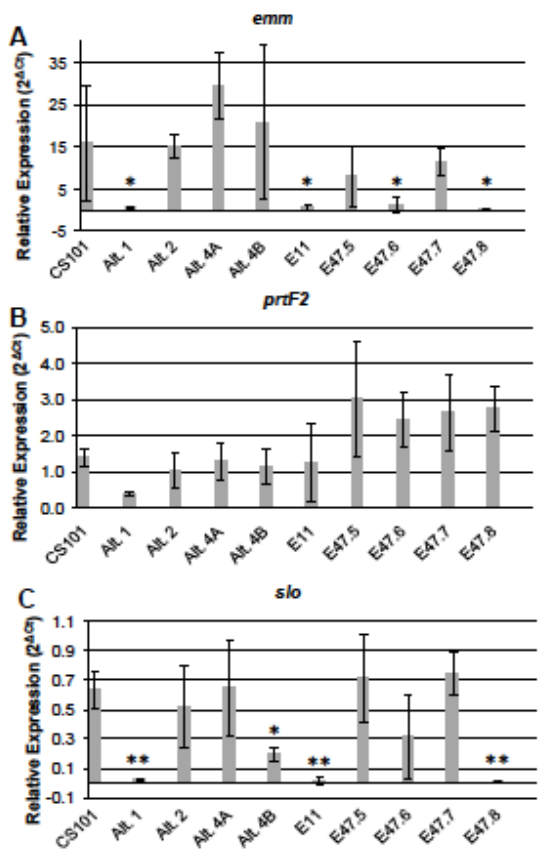


Figure 1. Virulence factor transcription varies between survivor strains. Parental strain CS101 and 9 survivor strains derived from CS101 were analyzed by real-time PCR for expression levels of three virulence factor genes (A) *emm*, (B) *prtF2*, and (C) *slo*. Alt strains were isolated from 14-week cultures of CS101 in TH broth. E11 and E47.5-E47.8 were isolated from 5-day co-cultures of CS101 with the A549 human lung epithelial cell line. The RNA was isolated from mid-exponential cultures in TH broth. Transcription of *proS* was used as a control and data are expressed as relative expression of the gene of interest to *proS* ($2^{\Delta Ct}$). The data shown is the average of 3 independent RNA isolations for each strain. The standard deviation is represented by the error bars. The values for the survivor strains were compared to CS101. (*) represents a significant difference of $p < 0.5$, and (**) represents a significant difference of $p < 0.05$. Primers for the virulence factors were generated for internal segments of each gene.

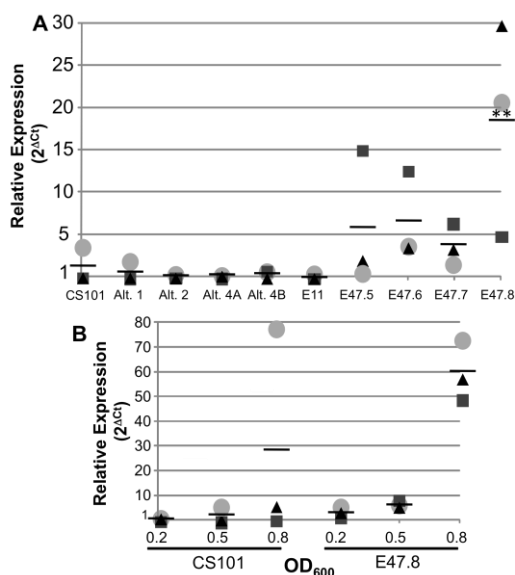


Figure 2. *speB* expression is variable and its expression increases in late exponential phase in survivor strain E47.8 and CS101. (A) Parental strain CS101 and 9 survivor strains derived from CS101 were analyzed by real-time PCR for expression levels *speB*. The RNA was isolated from mid-exponential cultures in TH broth. Transcription of *proS* was used as a control and data are expressed as relative expression of the gene of interest to *proS* ($2^{\Delta Ct}$). The data shown for each of 3 independent RNA isolations for each strain. The values for the survivor strains were compared to CS101. (**) represents a significant difference of $P < 0.05$. Primers for the virulence factors were generated for internal segments of *speB*. (B) Parental strain CS101 and E47.8 were analyzed by real-time PCR for expression levels of *speB* at OD_{600} 0.2, 0.5, and 0.8 representing early-, mid-, and late-exponential phase, respectively. The data shown for each of 3 independent RNA isolations for each timepoint.

Table 2: Survivor strains showed variable virulence in Zebrafish

Strain	Incidences of zebrafish death ^a					Mortality
	Day 1	Day 2	Day 3	Day 4	Day 5	
CS101	22	8				30/30
Alt. 1		1			3	4/12
Alt. 2		2				2/12
Alt. 4A	2	3				5/12
Alt. 4B		4				4/12
E11	1				1	2/12
E47.5	7	5				12/12
E47.6	3	7				10/12
E47.7	3	8				11/12
E47.8		1	1	2		4/12

^a 10^5 - 10^6 of log phase bacteria were injected intramuscularly into the dorsal muscle of the zebrafish.

Table 3: Attenuated survivor strains are cleared from Zebrafish spleens

	Spleen CFU ^a 24 hours	Spleen CFU ^a 3 days
CS101	2.5×10^4 (10/10)	Dead (5/5)
Alt. 1	12 (1/5)	1 (1/5)
Alt. 4A	1.5×10^4 (5/5)	16 (2/4) ^b
E11	5 (5/5)	0 (0/5)
E47.8	40 (5/5)	14 (1/5)

^a Spleens were homogenized and plated on CNA medium. The number in parenthesis represents how many fish have remaining CFU, and the average CFU is reported for those fish.

^b One fish died before harvesting the spleen

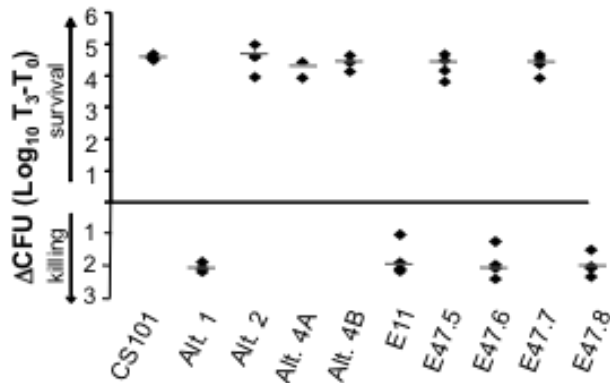


Figure 3. Whole blood killing varies between survivor strains. Heparinized human blood was collected from healthy donors. CS101 and the survivor strains were incubated at 37°C for 3 hours. Samples were taken at Time 0 and 3 hours for CFU enumeration. The data shows the change in CFU (T3-T0) for each of four donors, and the black bars represent the mean for each strain.

Research Project 17: Project Title and Purpose

Extended Chemosensitization with a Novel Small-Interfering RNA (siRNA) Sustained Release Nanosystem - The overall purpose of this project is to use the recent advances in nanotechnology to develop an effective and safe siRNA-based therapeutic strategy for drug-resistant ovarian cancers. Ovarian cancers are frequently resistant to standard chemotherapy. siRNA are a new class of therapeutic molecules that may provide a novel means to improve the effectiveness of chemotherapy; however, current use of siRNA for clinical purpose is largely limited by its short action, potential toxicity and inefficient delivery. This project will develop a novel platform that is capable of substantially prolonging the siRNA activity with reduced adverse effects. This may help translate this promising new treatment into a clinically useful form of treatment for a cancer that is normally refractory to the current standard drug therapy.

Duration of Project

1/30/2009 – 12/31/2009

Project Overview

Ovarian cancer is generally resistant to conventional chemotherapeutic agents. siRNA may improve the effectiveness of chemotherapy; however, current use of siRNA for clinical purpose is largely limited by its short action, toxicity and inefficient delivery. Our primary objective is to develop a novel siRNA platform to increase the responsiveness of ovarian cancer to chemotherapy for an extended period of time while causing minimal undesirable toxicity.

Aim 1. Formulate and characterize a polymer-lipid hybrid nanoparticle (PLN) as the platform for sustained siRNA release.

siRNA-PLN will be prepared and characterized for their physicochemical properties including particle size, surface charge, morphology, structure, siRNA loading, and stability. siGLO will be used as the primary model siRNA for studies in aim 1. The attached fluorescent moieties allow tracking of the siGLO distribution. Particle size and morphology of siRNA-PLN will be measured using photon correlation spectroscopy and electron microscope imaging methods. siRNA release and encapsulation will be spectrophotometrically evaluated using PLN loaded with siGLO. We also expect a high dependence of the drug loading and release properties of PLN to their internal structures. Differential scanning spectroscopy will be used to determine the structure of the PLN to test this hypothesis. Samples of PLN will be stored for weeks and the changes in particle size will be monitored to determine if significant aggregation or growth occurs, so the physical stability of the nanosystem can be tested.

Aim 2. Evaluate siRNA-PLN for its *in vitro* biological behaviors in cultured cancer cells.

siRNA-PLN prepared will be tested using SKOV-3 drug-resistant ovarian cancer cells. The SKOV-3 cell line has demonstrated strong resistance to chemotherapy drugs. In addition, animal models of SKOV-3 xenograft tumor are available, so continuity of work using the *in vitro* data is possible in the future. Using SKOV-3 cells, the intracellular sustained release kinetics, sustained protein and mRNA knockdown activity, and chemosensitization effect of siRNA-PLN will be extensively evaluated by fluorescent microscoping imaging, Western blot analysis and RT-PCR

techniques, respectively.

Principal Investigator

Ho-Lun Wong, PhD, BSc Pharm
Assistant Professor of Pharmaceutics
Temple University
3307 N. Broad Street
Room 433 Allied Health Professions Bldg.
Philadelphia, PA 19140

Other Participating Researchers

Hui-Yi Xue, PhD – employed by Temple University

Expected Research Outcomes and Benefits

PLN have been used for delivering several charged compounds with positive outcomes. We will take the challenge to move to molecular cancer therapeutics using this previously reliable system. We expect to achieve the following outcomes and benefits upon completion of this project:

- A novel siRNA-PLN system will be successfully developed with its physicochemical properties characterized. This system is physically stable after storage and in serum-supplemented medium.
- Control siRNA-PLN will induce lower non-specific toxicity compared to the conventionally used cationic liposomes, as a result the LD50 is significantly increased ($P < 0.05$ considered significant, same below).
- Sustained intracellular release of siRNA achieved, with the duration of effective siRNA activity doubled.
- siRNA remains biologically active. Significant knockdown of the targeted mRNA and protein will be observed compared to the negative controls.
- Significant chemosensitization to paclitaxel (> additive effect of paclitaxel alone plus siRNA alone) will be demonstrated in drug-resistant ovarian cancer cells treated with siRNA-PLN treatment as measured by viability assays and apoptotic assays. This chemosensitizing effect will last well over 72 hours.
- This will translate into a considerably larger time frame for the clinicians to administer the combinational chemotherapy, offering the much needed flexibility in treatment, reducing the need for multiple dosing, which further will save treatment costs and improve patient compliance.

Overall, the studies will generate the much needed data allowing us to apply the R21 grant regarding the *in vivo* use of this system. With the ability to suppress a low turnover protein, we may also use the siRNA-PLN as a key tool to perform various mechanistic studies and apply for the more mechanism-driven R01 grant.

Summary of Research Completed

1. Carrier formulation and characterization

A number of nanostructured carrier formulations were prepared and characterized. Carriers formulated include (1) carriers used for enzymatic degradation, e.g. lipid nanoparticles of solid triglycerides (TL, TM, TP, and TS), NLC of trimyristin containing different oil content (10 to 30%), and mixture of two triglycerides ; (2) carriers used for intracellular kinetics, immunoblotting studies and efficacy studies, e.g. nanocarriers loading rhodamine-siRNA or anti-survivin-siRNA (surv-siRNA).

The size and zeta potential values of these carriers were measured using photon correlation spectroscopy (PCS). Overall, the size of all nanocarriers prepared was around 200 nm, which increased to the range of 250-300 nm with siRNA loading. The single peak distribution (Fig. 1A) indicates no strong aggregation. The zeta potential values were around -20 mV (Fig. 1B), values typically suitable for stable dispersion of lipid particles using non-ionic surfactant. Selected NLC carriers (TM without siRNA, 10%, 20%, 30%) were incubated at 37° C for 72 hours in citrate buffer. Only slight increases in the size and polydispersity index were detected, and there was no significant changes in zeta potential ($P > 0.05$). The findings suggest that the carriers should remain generally stable under the experimental conditions used in the following studies.

2. Simulated LAL-mediated carrier degradation

Intracellular degradation rates of lipid carrier were studied in lysosomal acid lipase (LAL) system. A number of carrier parameters were evaluated and their effects on LAL-mediated degradation profiles were shown in Figure 2. The data of the two control groups (no LAL, and carrier made of cetyl alcohol which is not a substrate of LAL) show that most of the release of free fatty acids is the consequence of LAL-mediated degradation (Fig. 2A). Although the carriers with solid triglycerides of lower melting points (e.g. trilaurin and trimyristin) degraded modestly faster than those using higher melting point triglycerides (e.g. tristearin), the differences were not significant (Fig. 2A, $P > 0.05$). Mixing of two triglycerides with different melting points also did not affect the enzyme-degradation rates as well (Fig. 2B). It was found that only the liquid oil content significantly modified the carrier degradation rates. The higher the liquid oil content, the faster was the degradation (Fig. 2C). These differences in degradation rates were reflected by the quicker loss in the turbidity (Fig. 2D) when the high oil content carrier (e.g. 30%) was compared to the low oil content carrier (e.g. 10%). A nanostructured carrier with high oil content is likely less organized, and tends to open up to release the loaded siRNA more readily.

3. Simulated intracellular siRNA release kinetics

Three carrier formulations loading rhodamine-labeled siRNA were prepared for these studies. Their encapsulation efficiency values of 10% oil, 20% oil and 30% oil formulations were $76.2 \pm 6.1\%$, $81.0 \pm 5.7\%$ and $80.2 \pm 4.7\%$, respectively. As shown in Fig. 3, by manipulating the oil content in the nanocarrier (from 10 to 30%), the siRNA release rate could be modified. A positive correlation between the carrier oil content and siRNA release was shown. This trend was generally consistent with the lipid degradation data in Fig. 2C. The release was also slow without

the enzymatic action of the LAL, indicating that the siRNA release was a result of carrier degradation. A modest initial burst ($\approx 20\%$ in first 2 hrs) was observed in the “10% oil” group, indicative of some extent of surface adsorption of the siRNA molecules on the carrier. From the perspective of siRNA delivery, this is not necessarily counterproductive as it may provide a quick start of the RNAi action.

4. Extension of intracellular siRNA kinetics by nanostructured carriers

The “fast” (30% oil) and “slow” (10% oil) formulations were used for epifluorescence microscopy studies. Fig.4 shows time-changes in intracellular levels of siRNA (red) and lipid (green) delivered by 4 different formulations: fast-NC (top row), slow-NC (second row from top), DOTAP/cholesterol liposomes (third row from top) and proprietary (bottom row, Lipofectamine-2000, note no green fluorescence because there was no lipid added),. DRAQ5 (blue) was added to help locate the nuclei. For each formulation the images on Day 1, 3, 5 and 7 (from left to right) were shown here. Substantial intensities of siRNA (in red to orange-yellow) and lipid could be observed after 7 days in some cells treated with the slow formulation. In fast-NC group, siRNA could be detected after 5 days, but not after 7 days. In proprietary and liposome groups, spots of siRNA could be seen after 3 days but too weak to be detected after 5 days. The lipids of liposomes dissipated quickly (green color practically gone after 3 days). Our results demonstrate that manipulation of the nanocarrier properties can lead to shaping of intracellular siRNA kinetics for different profiles, and by doing so it is possible to stretch the normally brief presence of siRNA to 7 days or possibly longer.

5. Nanocarrier formulations modified and extended durations of survivin knockdown

We further evaluated the functionality of the surv-siRNA loaded nanocarrier. Survivin, a protein highly expressed in cancer cells was used as our model target. The survivin knockdown effect of surv-siRNA-nanocarrier was studied using Western blotting analysis. Results are shown in Fig. 5. Panel A presents the representative results of survivin and actin time-profiles after different treatments; panel B shows the quantitative analysis result of the survivin levels (mean + SD, N = 3 independent experiments). We demonstrated that: (a) Both fast and slow surv-NC formulations were able to substantially knock down survivin. The result indicates that the siRNA molecules encapsulated in this new type of nanocarrier remained functional. (b) Both carrier formulations extended the survivin knockdown compared to when the siRNA was delivered using Lipofectamine-2000 and DOTAP/ cholesterol liposomes. Knockdown (to $< 25\%$ of the base level) period was stretched from 3 days to 5 days with fast-surv-nanocarrier and to 9 days using slow-surv-nanocarrier. Our findings show that the controlled siRNA release design of nanocarrier can effectively function in a biological system to achieve the desired therapeutic effect in a sustained manner.

6. Sustained survivin knockdown translated into extended chemosensitization

It was shown that survivin knockdown was able to restore the sensitivity of cancer cells to anticancer chemotherapy agents. We performed MTT assays (Fig. 6) to determine if extended chemosensitization could be obtained using the surv-siRNA-nanocarrier systems. In the upper panel, pretreatment of cancer cells with 50 nM surv-siRNA lead to reduction of the IC₅₀ value

of docetaxel from 0.78 nM to 0.18 nM (i.e. from normal to chemosensitized state). We then treated the cancer cells with 0.18 nM at different times after the cells were pretreated with different formulations of surv-siRNA. The lower panel of Fig. 6 shows that the cells remained in chemosensitized state (i.e. \approx 50% cell kill) for 9 days and 5 days in the slow- and fast-surv-nanocarrier groups, respectively, *versus* 3 days in the standard Lipofectamine-2000 treatment. This essentially tripled the effective chemosensitization time-window. The results are consistent with the intracellular kinetics and survivin knockdown profiles.

7. Overall conclusion and Milestones

In these series of studies we have demonstrated that by manipulating the composition of a solid-lipid based nanocarrier design, the intracellular release kinetics of a macromolecules such as siRNA can be conveniently modified and sustained. This opens up the possibility of scheduling more convenient weekly dosing regimens of chemo-siRNA-therapy treatment of cancer.

In addition, based on these data: (1) two abstracts have been submitted to AAPS (American Association of Pharmaceutical Scientists) for poster presentation in their annual meeting in Nov 2010 (under review); (2) A manuscript has been prepared and will be submitted to the Journal “Biomaterials” in late May; (3) and an application made in February 2010 for the R01 grant from the NIH.

Figure 1

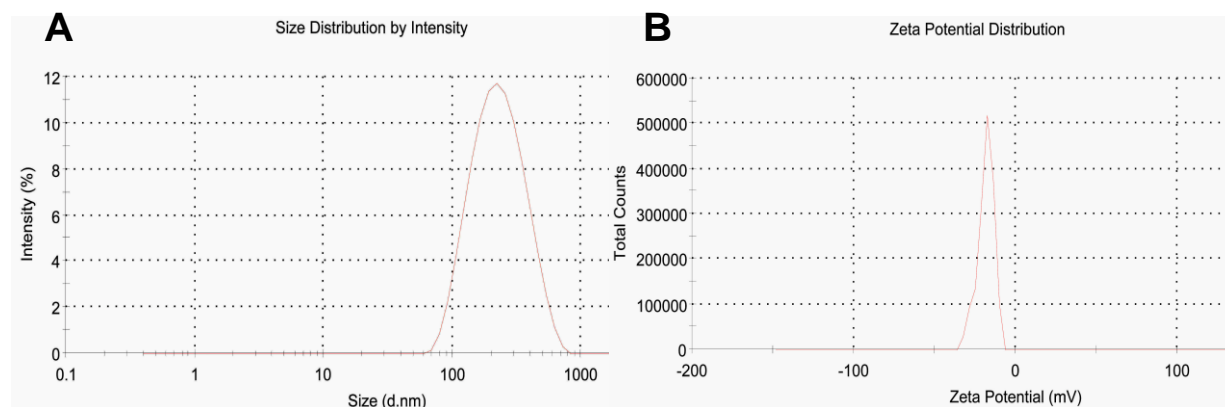


Figure 2

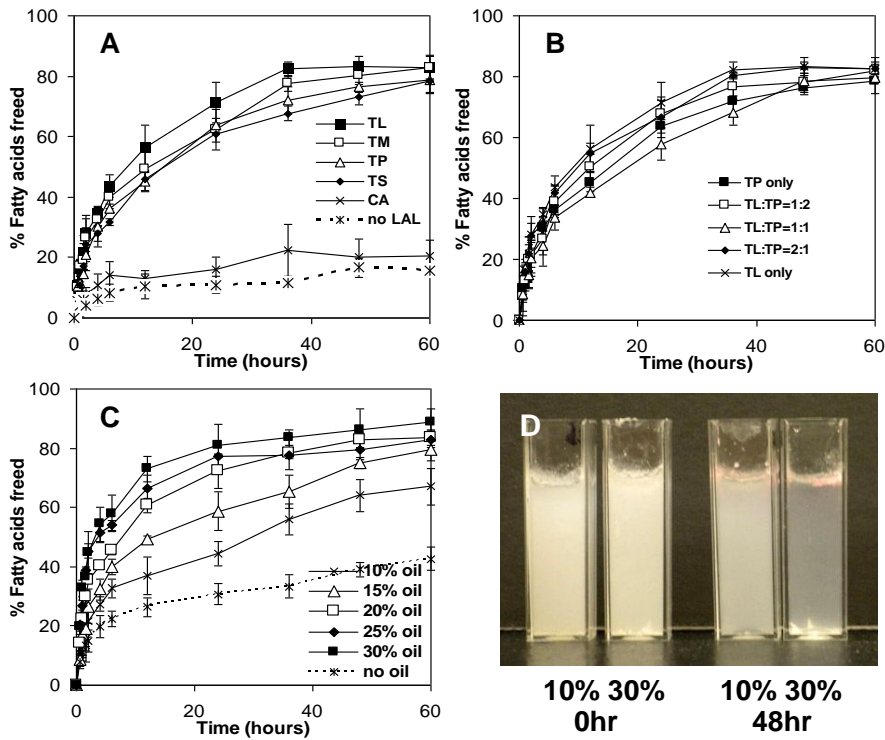


Figure 3

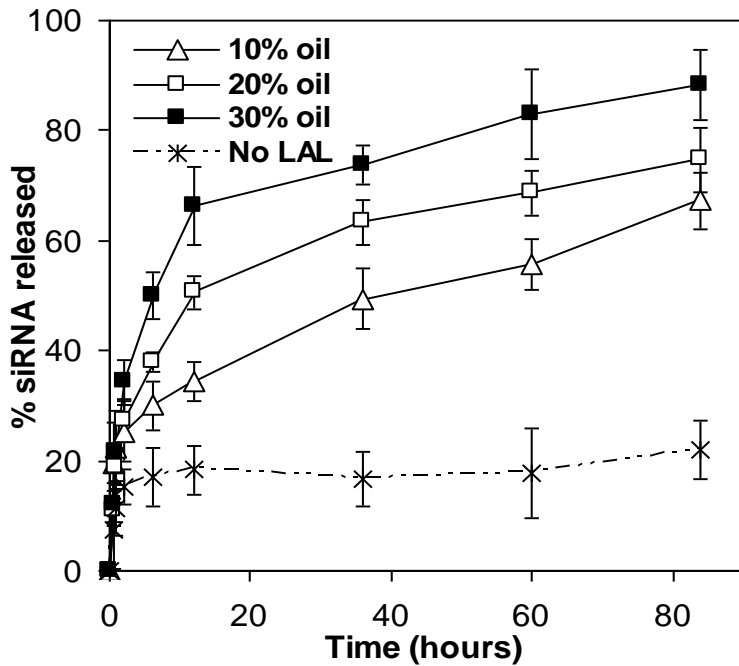


Figure 4

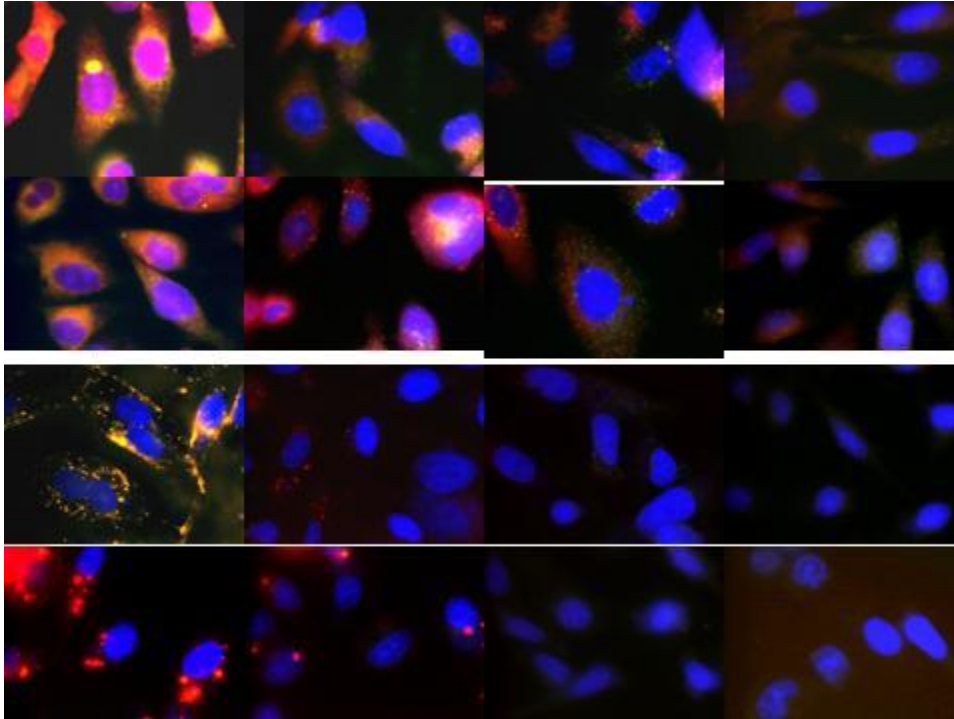


Figure 5

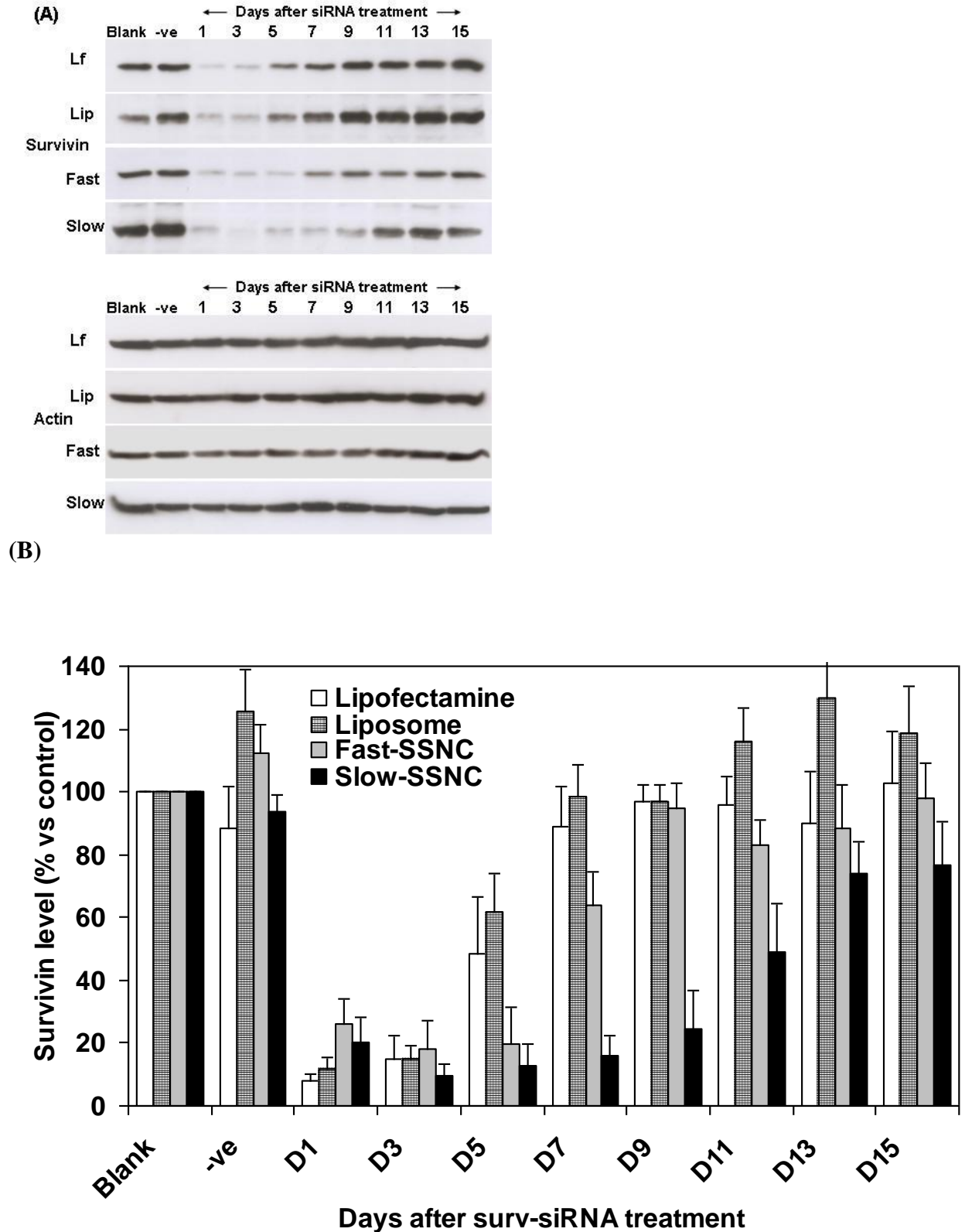
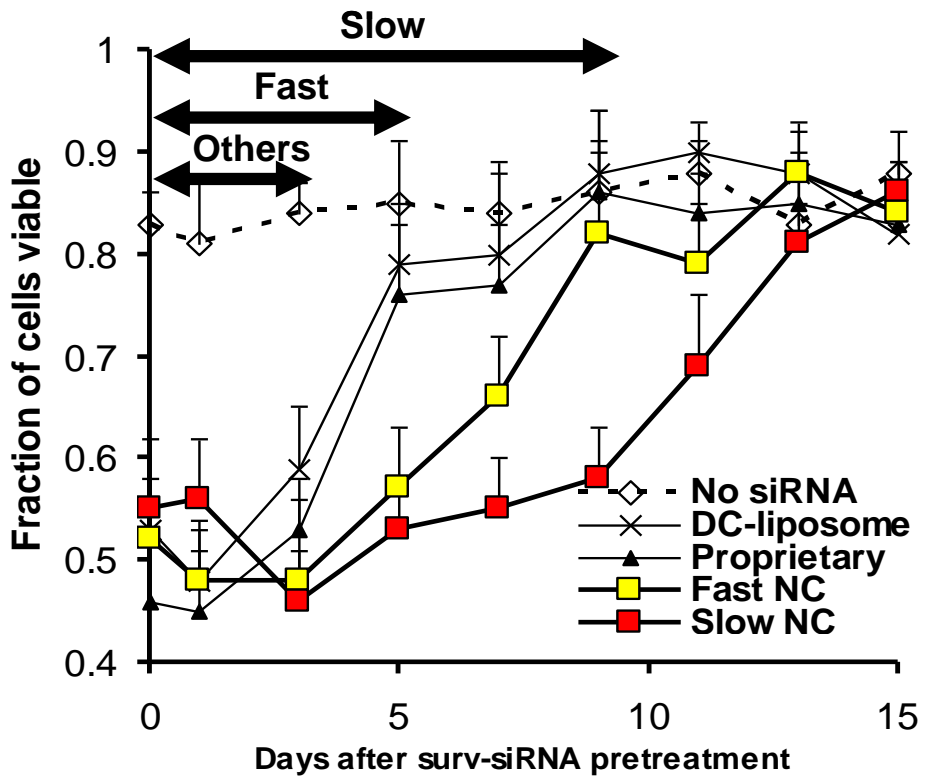
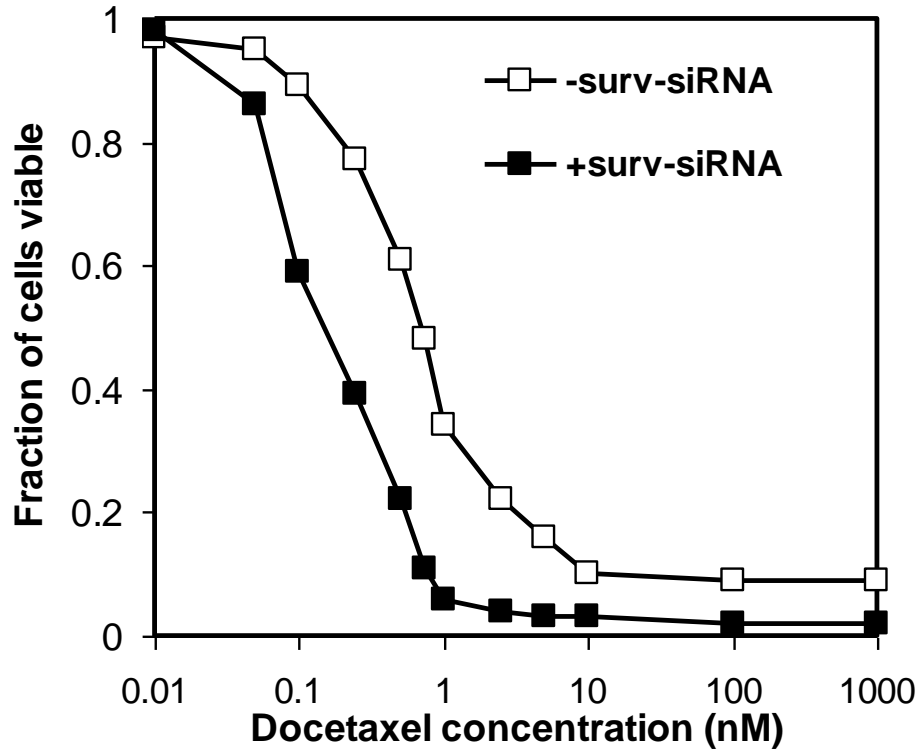


Figure 6



Research Project 18: Project Title and Purpose

Using an IVR-Cellular Telephone System to Improve Outcomes in Chronic Obstructive Pulmonary Disease - We intend to extend our findings of reducing the incidence and severity of Chronic Obstructive Pulmonary Disease (COPD) exacerbations by using a PDA-computer based management system to one that uses an *interactive bidirectional cell or land-based phone technology*.

Anticipated Duration of Project

1/30/2009 – 12/31/2011

Project Overview

In this project, we intend to extend our findings of reducing the incidence and severity of COPD exacerbations by using a PDA-computer based management system to one that uses an *interactive bidirectional cell or land-based phone technology*. Our primary specific aim is that that this method will *decrease the time to the first COPD exacerbation*. Our secondary specific aims are that we believe that this method will: 1) *enhance patient acceptance of self monitoring*, 2) *improve communication between patients and providers*, and 3) *provide a platform for the generalization of our management paradigm to the COPD patient population at large*. Finally, we intend to use the information from this pilot project as preliminary data to: 1) *submit an application via the NIH RO1 funding mechanism to demonstrate that this method decreases the frequency of COPD exacerbations in a multicenter prospective and randomized 1- year trial and;* 2) *prepare a proposal to the PA-DOH Medical Assistance program to pilot this program as a disease management program for COPD patients having repeated hospital admissions, thereby reducing the costs and morbidity of repeated COPD exacerbations*.

Principal Investigator

Gerard J. Criner, MD
Professor of Medicine
Temple University
3401 N. Broad Street
785 Parkinson Pavilion
Philadelphia, PA 19140

Other Participating Researchers

Francis Cordova, MD; Alfred Bove, MD – employed by Temple University
Ted Hoobler – employed by Insight Telehealth Systems

Expected Research Outcomes and Benefits

Although this project is designed as a proof-of-concept study, we will track all hospital admissions and exacerbations of either COPD as a measure of efficacy. Data from previous

studies in our center on similar populations will provide a basis for historical controls. Based on our Web-based telemedicine studies, we expect to find a reduction of hospital days and a reduction of acute exacerbations of COPD.

Summary of Research Completed

The telemedicine program is being expanded to include a larger COPD population. Temple University Hospital has approved this program to be used as a COPD disease management program under administration of the hospital.

The telemedicine system is undergoing revisions for the development:

- Online documentation of interventions
- Online documentation of physician interventions check
- Automatic fax transmission patient symptom alerts and interventions to the patients' physicians

In the period which is the subject of this report, InSight Telehealth System worked to adapt and build the current COPD disease management module. The process was straightforward once the clinical work flows and data management requirements were identified. New servers were brought online and a unique toll-free number was established for patients to report their daily symptoms. A COPD IVR script was recorded and programmed so that patients could now use their phones to enter data either from making a call, or by responding to a preprogrammed call. Phone messaging was also set up so that patients could leave messages for clinicians to respond to later either via text-to-voice or via the Internet. A highly secure site was created so that patients could communicate with their providers over the Internet should they choose to do so. Patients have the option of using either or both modes of communication. COPD-related risk scores were implemented based on a specific COPD patient baseline settings, and a function enabling text alerts to the On Call provider in the event of a risk score exceeding set values was added to the system. Functions for Progress Notes relating to each patient were established as was a specific area in which clinicians could make notes when prescribing medications. Many of the newer features and functions implemented are designed to facilitate the clinicians' focus on health care by providing a toolset that programmatically creates a highly secure archive of all activities in a central repository. A highly sophisticated next generation of the COPD program in which best practices has been programmed into an Intervention function is very close to release. It includes a smart phone-based Physician Orders function that enables on call physicians to be alerted to new patient medication requirements, make adjustments, and then alert nurses that changes have been ordered, all with a fully automated, secure archive trail.

We submitted an abstract on the telemedicine program in November 2009, which will be presented at the American Thoracic Society's annual Scientific Meeting, May 14, 2010 in New Orleans, Louisiana.

We have previously shown that daily monitoring of COPD symptoms and early intervention decreases the frequency and severity of acute exacerbations. Our pilot study suggests that the Temple COPD_{phone} with option of Internet contact is well accepted by patients. Patient compliance and the utility of the newer technology by patients and operating staff have not been reported.

COPD patients with prior AECOPD hospitalization or chronic use of oxygen were recruited. Patients were instructed to report their daily respiratory symptoms (dyspnea, sputum, coughing, wheezing, nasal congestion, fever, and sore throat) and peak flow using either a cell or land-based phone or via a HIPPA compliant password protected Internet website. Specialized nurse personnel used the real-time Website to view symptoms and either read or listened to subject messages. Staff entered interventions or messages via the computer that were translated to phone voice messages or real-time text emails after consultation with a pulmonary specialist about each patient's symptoms and planned interventions. The amount of time spent to review daily data and initiate appropriate interventions were reported as daily screening and intervention times, respectively. Compliance was calculated as actual/expected reporting of daily symptoms. Data are reported as mean \pm SD.

Forty subjects (age 65.8 yrs, FEV₁% 35 \pm 17, smoking pack years 43 \pm 21, 56% female, 21% African American) were enrolled. The mean duration of follow-up was 169 \pm 161 days with 8 and 4 patients > 12 and 6 months follow-up, respectively. The total number of patient days analyzed using Temple COPD_{phone} totaled 6,671. Overall COPD patient compliance was 89% \pm 11 for reporting daily symptoms. Fifty-five percent of patients transmitted their daily symptoms by phone, 20% by the Internet, and 25% by both phone and the Internet. The average number of patients reporting daily was 29 \pm 4 with 25% (7 \pm 2) of the patients requiring additional treatments (prednisone, antibiotics, or both) for AECOPDs. During follow-up, 17 patients had 0-1, 14 had 2-4, and 9 had > 5 AECOPDs. The average staff time/day to review daily patients' reported symptoms was 142 \pm 56 min (review time 30 \pm 3 min; intervention time 93 \pm 44), for approximately 5 min of staff time per patient.

The Temple COPD_{phone} Program with Internet-based capability provides a versatile tool for reporting daily AECOPD symptoms in a large cohort of patients with high daily compliance and an efficient use of specialized professional time. The economic impact of the program needs to be studied further.

Research Project 19: Project Title and Purpose

Immunotherapeutic Strategies for Alzheimer's Disease - A promising and understudied animal model of Alzheimer's disease (AD) is the cholesterol-fed rabbit. In the last three years, we replicated the demonstration that a rabbit model of AD carries a number of AD neuropathologies and is impaired in associative learning and extended the AD rabbit model to the domain of therapeutics by demonstrating efficacy of galantamine (Razadyne™) in ameliorating learning impairment in these rabbits. Whereas drugs such as Razadyne™ treat cognitive impairment in AD, their efficacy is modest. Immunotherapy may have the potential to prevent the development of AD in later life as well as to treat and reverse symptoms. Using AD model rabbits, we aim to test immunotherapeutic strategies that will maximize humoral (antibody) immune responses while minimizing proinflammatory responses.

Anticipated Duration of Project

1/30/2009 – 12/31/2010

Project Overview

Our initial data indicate that immunization of cholesterol-fed and control rabbits with β -amyloid ($A\beta$) had efficacy when administered beginning 6 or 8 weeks after the cholesterol/copper diet was initiated. However, the data on the timing of onset of $A\beta$ and other Alzheimer's disease (AD) neuropathology in the AD rabbit model are limited. We need to determine if we can prevent or reduce $A\beta$ and other AD neuropathology using $A\beta$ immunotherapy. Therefore, *Specific Aim 1* will characterize the development of neuropathology over a 10-week period of cholesterol/copper diet. *Specific Aim 2* will determine whether a noninvasive behavioral measure is associated with onset and development of AD neuropathology. *Specific Aim 3* will focus on the development of efficacious immunotherapeutic strategies as well as the optimal timing of immunotherapy using behavioral- and neuropathological-dependent measures. Our goal is to design an immunization strategy that promotes antibody responses through preferential differentiation and enhanced survival of helper T cells (T_H2) in lieu of T_H1 cells that produce proinflammatory cytokines.

Alzheimer's Disease Rabbit Model. Young (3-4 months) male New Zealand white specific pathogen free (SPF) rabbits and female retired breeder will be tested. *Dietary Regime.* Rabbits will be fed for 10 weeks (or the number of weeks specified in the research design) with 160 g/day of a commercially produced diet (Test Diet 7520) of 2% cholesterol added to Purina Mills High Fiber Diet. Control rabbits will be fed 160 g/day of Purina Mills High Fiber Diet. For experimental rabbits, 0.12 mg/liter copper sulfate will be added to distilled drinking water. Control rabbits will receive distilled drinking water.

Specific Aim 1. A total of 40 rabbits (20 young adult males, 20 retired breeder females a minimum of 24 months old) will be studied to characterize AD pathology development during the period that the animals are fed the cholesterol/copper diet. Brains will be examined for pathology in sections in frontal, temporal, parietal, and occipital cortex, hippocampus, and cerebellum and stained with H & E and immunostained for $A\beta$, tau, apoptosis, and gliosis.

Specific Aim 2. The same 40 rabbits used in Aim 1 will receive five days of training in eyeblink classical conditioning five days before they are euthanized. Training will follow procedures approved by the Temple IACUC and reported previously for AD model rabbits. After training is completed, rabbits are euthanized, perfused through the heart, and brains are collected for histology as described above.

Specific Aim 3. Based upon the neuropathology profile of young male and retired breeder female AD model rabbits (Aim 1), we will begin immunizing cohorts of AD model rabbits with β -amyloid 1-42 peptide ($A\beta_{1-42}$). Animals will be divided into two experimental adjuvant cohorts to allow us to compare: (1) conventional Freund's adjuvant; and (2) VIP anti-inflammatory neuropeptide. Moreover, we will assess the efficacy of prophylactic immunotherapy using these adjuvant regimes as well as immunotherapy efficacy at two time points post-pathology onset.

Principal Investigator

Diana S. Woodruff-Pak, PhD
Professor of Psychology
Temple University
1701 N. 13th Street
Weiss Hall
Philadelphia, PA 19122

Other Participating Researchers

Richard Coico, PhD, Joanne Manns, PhD, Kevin Brown, PhD, David Comalli, BA, Alexis Agelan, DVD, Christina Leuzzi, BA, Kim Nguyen, BA, Christina Shriver – employed by Temple University

Expected Research Outcomes and Benefits

Immunotherapy may have the potential to prevent the development of AD in later life as well as to treat and reverse some of its symptoms in AD patients. The rabbit model of AD, arguably the most valid of all existing animal models of AD, has not been used to test immunotherapeutic strategies, yet the rabbit has a close amino acid sequence to human A β . The concurrent risk of AD and cerebrovascular dementia, cardiovascular disease, diabetes, and other age-related chronic diseases make the rabbit model of AD a promising shared resource among investigators at Temple University School of Medicine. In addition to studies of immunotherapy, tissues from AD model rabbits could be used as a Core bioresource for a Program Project proposal focusing on Alzheimer's disease and related disorders. Thus, this proof-of-concept proposal using the AD rabbit model has significant translational potential for treatment and prevention of AD in humans. By extension, this potentially high impact work would position Temple University as a major contributor to the global research effort to quell the morbidity and mortality associated with neurodegenerative diseases such as AD.

Summary of Research Completed

Overview: Building on our previous replication and extension of the hypercholesterolemic rabbit as an animal model of AD to test therapeutic applications, we demonstrated that immunization of cholesterol-fed and control rabbits with β -amyloid (A β) had efficacy when administered beginning 6 or 8 weeks after the cholesterol/trace copper diet was initiated (Woodruff-Pak, Manns, Nguyen and Coico, submitted). Specific Aim 1 of this project is directed at the timing of pathology onset and progression because data on the timing of onset of A β and other AD neuropathology in this model are limited. Initial analyses of the first study designed to address Aim 1 indicate that A β is present four weeks after initiation of the cholesterol/trace copper diet but not two weeks after diet initiation. Analyses are in progress for the second study addressing this aim. Specific Aim 2 addressed a functional (behavioral) outcome measure of immunization, eyeblink classical conditioning. Eyeblink conditioning is severely impaired in AD in humans, but two separate studies in this project demonstrated that inoculation against A β does not ameliorate impaired eyeblink conditioning in AD model rabbits. Specific Aim 3 focused on the

development of efficacious immunotherapeutic strategies and the optimal timing of immunotherapy. We found that initial immunization with 0.5 ml of A β ₁₋₄₂-peptide conjugated to keyhole limpet hemocyanin (KLH) in PBS mixed with 0.22 ml of Freund's complete adjuvant followed by boosts every two weeks with 3 or 4 additional doses of A β ₁₋₄₂-KLH in Freund's incomplete adjuvant effectively reduced A β levels in inoculated AD model rabbits. Analyses of results testing the timing of inoculations are in progress.

Specific Aim 1: Pathology Onset and Progression: Two studies were carried out to address this aim -- one with a sample size of 8 animals to compare pathology after 4 and 10 weeks on the cholesterol/trace copper diet and one with a sample size of 25 animals to examine pathology development in 2 AD model rabbits at weekly intervals between the second and tenth week on the diet.

Pathology Study 1. Characterization of neuropathology (CAA, intra- and extracellular A β) in at 4 weeks and in fully induced animals at 10 weeks. *Rabbits.* 8 3-4 month SPF male New Zealand white rabbits were purchased from Covance (Denver, PA). Rabbits were housed individually and had 24 h access to rabbit chow and water and had a 12/12 h light/dark cycle. Daily rations of food for 2 AD model rabbits were weighed, packaged in zip-lock bags, individually labeled, and stored in separate bins. Rabbits were fed with 160 g/day of a commercially produced diet (Test Diet 7520) of 2% cholesterol added to Purina Mills High Fiber Diet. Copper sulfate (0.12 mg/liter) was added to distilled drinking water. Two rabbits were treated with the cholesterol/copper regimen for 4 weeks and 2 were treated for 10 weeks. Four SPF male New Zealand white rabbits were control animals. Control rabbits were fed Purina Mills High Fiber Diet and distilled water ad lib and euthanized.

METHODS: A β and CAA Immunohistochemistry. Brain tissue was blocked, processed, and embedded in paraffin. Sections of 4 μ m in thickness from representative areas of the brain, including the frontal and temporal cortex including hippocampus were cut on a microtome (Leica RM 2135) and placed on electromagnetically charged slides. Immunohistochemistry was performed using techniques we reported previously (Woodruff-Pak, Agelan, and Del Valle, 2007).

Quantitative Analysis of Histopathology. A PaxCam3 Digital Camera System (MIS, Villa Park, IL) interfaced with a Nikon LabPhot microscope and a PC was used to analyze images photographed using a Plan Apo 20x objective. Optical digital analysis software was used to identify specified saturation and pixel densities in selected areas (PaxIt Enhanced Measurement/Image Analysis Module, MIS, Villa Park, IL). A consistently sized region of interest was used for analysis and calibrated for measurement in μ m. The amount of pathology (intercellular A β , CAA) in a representative selected field in temporal cortex that included hippocampus was measured. The fields compared between rabbit brains were always of equal size. The software highlighted the selected pixels marking the pathology on the computer screen and then calculated the area. Once the quantification was completed, the values were saved in Excel, transferred to SPSS and statically analyzed by treatment group (SPSS version 16).

RESULTS: CAA. Examples of CAA cortical and leptomeningeal vessels and our quantification methods are shown in Figures 1 and 2. Comparisons were made of CAA in cortical (Figure 3) and leptomeningeal (Figure 4) vessels in three groups of rabbits: 4- and 10-week induction and

control. The sample sizes were too small to yield statistically significant results, but the quantification indicated that there was a tendency for there to be a progression of pathology from 0 exposure to the cholesterol/copper regimen to 10 weeks of exposure (Figures 3 and 4). A β . Intracellular A β 40 (Figure 5) and A β 42 also showed some increase with increasing time on the cholesterol/copper regimen (Figure 6).

Pathology Study 2. Characterization of neuropathology (CAA, intra- and extracellular A β) developing between 2 and 10 weeks. Table 1 shows the research design of this study. Methods were the same as described for Pathology Study 1 above, but 25 young male rabbits were tested. All rabbits arrived at our facility at the same time and were 3-4 months of age. Two were control rabbits fed a normal diet and 23 were initially administered a normal diet until they were put on the cholesterol/trace copper diet at various intervals indicated on Table 1. Control rabbits were euthanized 8 weeks after initiation of the study, and the rest of the rabbits were euthanized at the same time after 12 weeks. All data have been collected for this study, and the lengthy histological analyses are underway.

Specific Aim 2: Eyeblick classical conditioning in immunized versus non-immunized AD model rabbits. In our report of the period covering Jan-June 2009, we described research addressing this aim and demonstrating both in young male ($n = 25$) and retired breeder female ($n = 26$) AD model rabbits that immunization against A β did not ameliorate impaired eyeblink classical conditioning. Although intracellular A β was significantly reduced in both young and older inoculated AD model rabbits, behavioral impairment was not reversed.

A second study carried out in this funding period (described below for Aim 3) was designed to address timing of inoculation effects. There were no differences in acquisition of eyeblink classical conditioning (Figure 7).

Specific Aim 3: Timing of effective inoculations. In previous studies we demonstrated efficacy of inoculations initiated 4, 6, and 8 weeks after onset of cholesterol/trace copper regimen. In this study we inoculated rabbits before the dietary regimen began. A total of 20 rabbits were tested, and 10 received A β immunizations before the initiation of the diet. The research design of this study is shown in Table 2. As mentioned previously, eyeblink classical conditioning results confirmed the two previous studies reported for Specific Aim 2 -- inoculations did not ameliorate impaired conditioning. Histological analyses of the data have been initiated.

Table 1. Research design and sample size of second pathology study. Beginning in two weeks after the 4-month-old rabbits arrived, 2 or 3 rabbits were started on the cholesterol/trace copper diet for the remainder of the study. This design yielded rabbits treated with the diet for 2, 3, 4, 5, 6, 7, 8, 9 and 12 weeks.

Weeks	Number of AD Rabbits	Number of Control Rabbits 2
1	0	
2	3	
3	2	
4	3	
5	2	
6	3	
7	2	
8	3	
9	2	
10	0	
11	0	
12	3	
TOTAL	23	2

Table 2. Research design of study addressing the timing of inoculation. There were 10 rabbits/group for a total of 2 groups - A β 1-42-KLH inoculation versus no inoculation. There were four inoculations BEFORE initiation of the cholesterol/copper diet.

Time Line

Week	Treatment
Rabbits arrive	No treatment
1	Inoculation 1
2	
3	
4	Inoc. 2
5	
6	Inoc. 3
7	
8	Inoc. 4
9	Euthanize 2 rabs/group
10	Begin Diet-wk 1
11	Diet Wk 2
12	Diet Wk 3
13	Diet Wk 4
14	Diet Wk 5
15	Diet Wk 6
16	Diet Wk 7
17	Diet Wk 8
19	Diet Wk 9-eyebcond
20	Diet Wk10-eyebcond
21	Euthanize

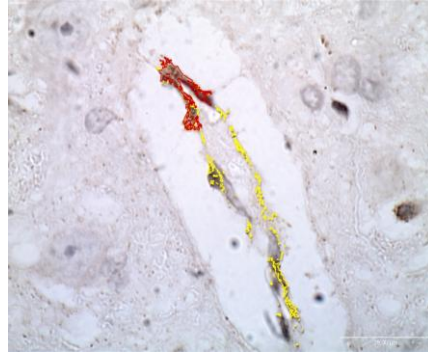
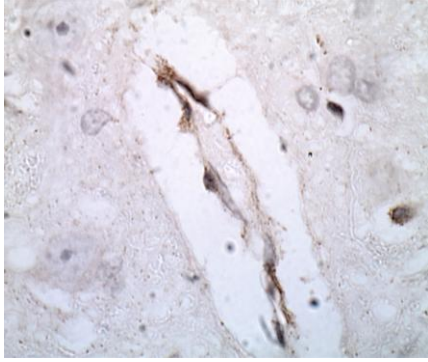


Figure 1.

LEFT: Cortical vessel near the hippocampus, 10-week induced AD model rabbit.

RIGHT: Aβ40 measured with restricted ROI. (100x)
The pixels stained for Aβ40 are masked in colors from the quantification

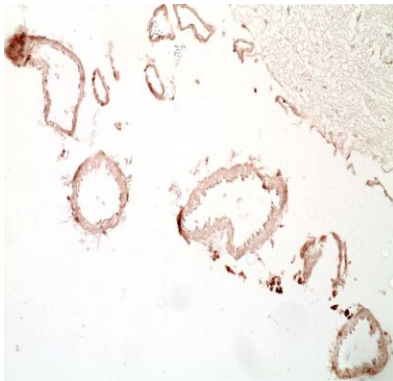


Figure 2.

LEFT:
Leptomenigeal vessels at temporal periphery, 4-week induced AD model rabbit.

RIGHT: Aβ40 measured with restricted ROI. (20x)
The pixels stained for Aβ40 are masked in colors from the quantification software.

Figure 3. BELOW LEFT: Quantitative assessment of expression of A β 40 and 42 in cortical vessels in 2 rabbits fed a regimen of cholesterol and copper for 0 (Control), 4, or 10 weeks.

Figure 4. BELOW RIGHT: Quantitative assessment of expression of A β 40 and 42 in leptomenigeal vessels in 2 rabbits fed a regimen of cholesterol and copper for 0 (Control), 4, or 10 weeks.

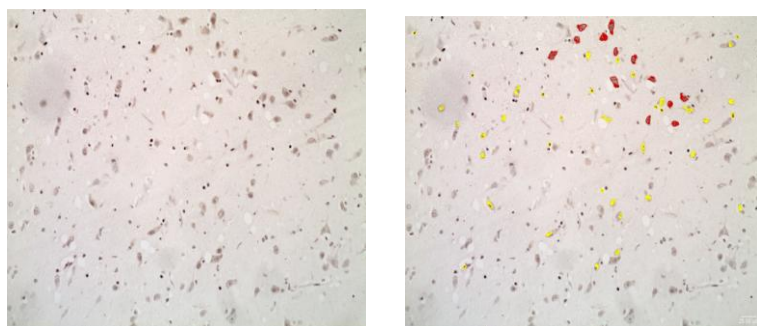
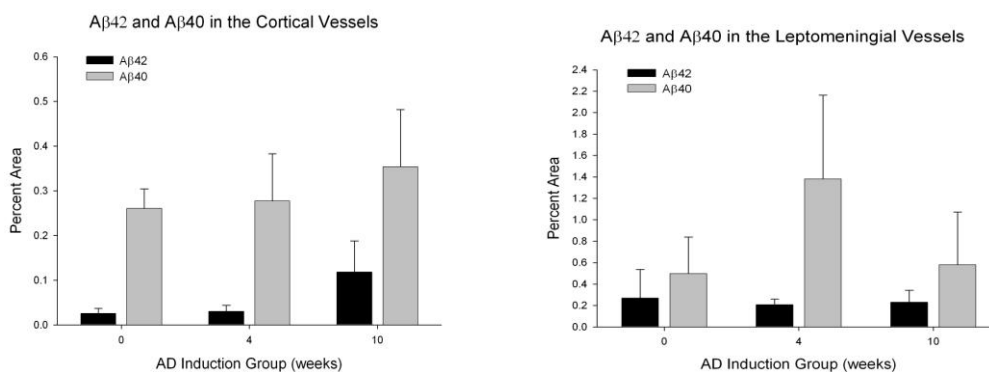


Figure 5. Intracellular expression shown in temporal parenchyma in 10-week induced AD model rabbit. **RIGHT:** A β 40 measured with maximum area ROI (20x). The pixels stained for A β 40 are masked in colors from the quantification software.

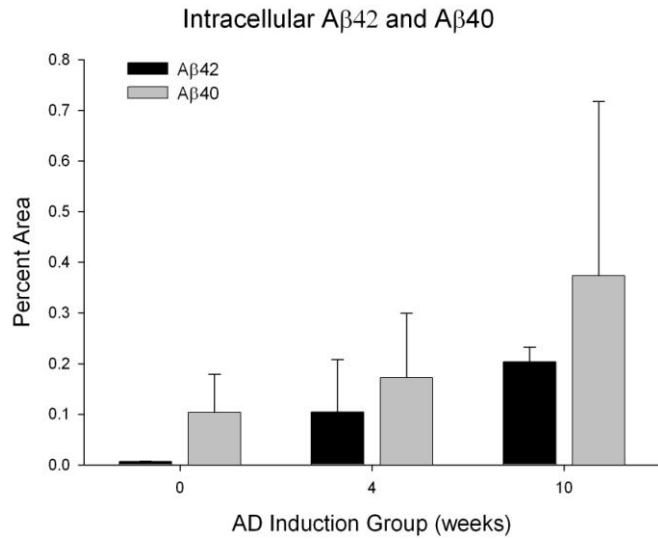


Figure 6. Quantitative assessment of intracellular expression of Aβ40 and 42 in 2 rabbits fed a regimen of cholesterol and copper for 0 (Control), 4, or 10 weeks.

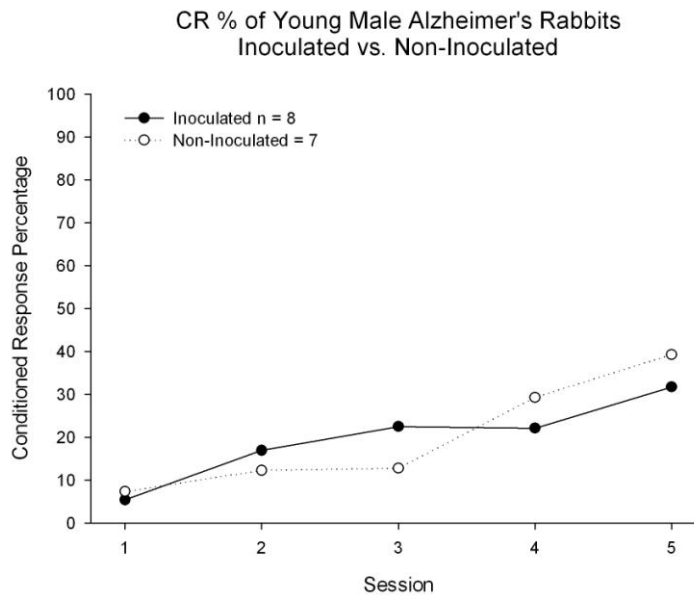


Figure 7. Acquisition over five 90-trial sessions of eyeblink classical conditioning in AD model rabbits that received four inoculations before initiation of a 10-week cholesterol/trace copper diet. Rabbits were tested eight weeks after initiation of the cholesterol/trace copper diet.

Research Project 20: Project Title and Purpose

*Improving Biomedical Informatics Support at Temple Health Sciences Center - An increasing number of basic and clinical studies at Temple University require merging and analyzing a large volume of biomedical data collected from a variety of sources. Mastering appropriate informatics skills is one of recognized current challenges and is at the forefront of personalized medicine development. The purpose of the project is to provide informatics support within Temple Health Sciences Center (THSC) that will correct interoperability among existing clinical, molecular and other data resources and allow more efficient and potentially more accurate inference for the purpose of understanding disease states and pharmacotherapies. In particular, we propose *developing effective tools for biomedical data management, retrieval and data mining and providing informatics and analytical help as to efficiently support comprehensive translational research within THSC.**

Anticipated Duration of Project

1/30/2009 – 12/31/2010

Project Overview

Aim 1: Providing data management support for integration of genomic, molecular, and clinical information and creating framework for mining integrated biomedical data.

Implementation:

(a) *Developing and hosting biomedical websites:* Experience gained on developing and hosting DisProt and a dynamic website will be used towards developing and hosting biomedical websites to promote and facilitate research at other THSC laboratories.

(b) *Providing access to external biomedical data:* Data of interest to THSC investigators will be extracted from external genome, proteome, genotype, bioinformatics and other public biomedical data repositories.

(c) *Developing a data warehouse:* Given multiple databases our objective will be to develop a data warehouse that allows investigators to securely query de-identified data stored at these systems. Data from the clinical, administrative, molecular and other systems will be transformed and loaded into the repository.

(d) *Developing advanced analysis tools for constructed data warehouse:* Various data mining methods will be implemented to support knowledge discovery in the constructed data warehouse. State of the art methods will be implemented for association analysis, cluster analysis and anomaly detection.

Aim 2: Continuing expired bioinformatics support and introducing additional bioinformatics services at THSC aimed at expanding into clinical and translational medicine.

Implementation:

(a) *Providing access to bioinformatics and other analytical software:* Access and training will be provided to various bioinformatics software tools related to sequence database, analysis, and management, pathway analysis, protein structure prediction, analysis and visualization.

(b) *Analysis of protein structure:* We will analyze amino acid sequences to predict if a protein is fully ordered or it is likely to contain intrinsic disordered regions. For ordered proteins, we will predict their structure using tools developed elsewhere, while protein disorder will be characterized using our own methods.

(c) *High throughput data analysis:* Steps to be supported for a typical gene expression study include (i) Image processing; (ii) Identification of differentially expressed genes; (iii) Control of false discovery rate; and (iv) Pathway analysis.

(d) *Fusion of clinical, molecular and environmental data.*

Principal Investigator

Zoran Obradovic, PhD
Director, Information Science and Technology Center and Professor Computer and Information Sciences Department
Temple University
303 Wachman Hall
1805 N. Broad St.
Philadelphia, PA 19122

Other Participating Researchers

None

Expected Research Outcomes and Benefits

The project will immediately result in a much stronger informatics component of the Keystone Biomedical Informatics Resource and so will benefit a Clinical and Translational Science Awards grant proposal currently in preparation by a large group of investigators from Temple Health Sciences Center jointly with collaborators at Fox Chase Cancer Center and Geisinger Health System.

Other expected outcomes in the next 2-year period will include informatics support for ongoing and planned projects at Temple Health Sciences Center that have bioinformatics tasks defined within their specific aims.

Summary of Research Completed

In this period we have continued some collaborations with basic medical, clinical and translational projects within Temple Health Sciences Center and established several new

collaborations. The results of work in the July 2009 – June 2010 period are summarized in this section.

Analysis of Regulatory Elements in Maternal mRNA Sequences

In the July 2009 – June 2010 period we continued cooperation with Dr. K. Latham's group, the Temple Fels Institute for Cancer Research and Molecular Biology, aimed at researching various aspects of control for recruitment of stored maternal mRNAs (MmRNAs). This year we expanded enrichment analysis on Bag4 and Fmnl3 3'UTRs to include searching for not only the exact matches of potential motifs, but also for matches with a certain number of mismatched nucleotides.

After Dr. Latham's group provided a shorter list of candidate motifs, we performed analysis that focused on possible evidence of co-regulation. We tested how often these candidate motifs occur together in groups of two, three and more, and provided statistical significance for all such events.

We predicted secondary structure of all 3'UTR sequences involved in previous analyses. We then helped Dr. Latham's group perform a wide-scale analysis of predicted secondary structures to test several hypotheses of relationship between the position of candidate motifs in 3'UTRs and the secondary structure of those sequences.

This study produced one doctoral thesis in Dr. Latham's group and a paper submission to AJP - Cell Physiology that is currently under review.

Large Scale Correlation Analysis of Gene Expression and DNA Methylation Data in Placenta and Cord Blood

Jointly with Dr. Carmen Sapienza at the Temple Fels Institute for Cancer Research and Molecular Biology we have examined DNA methylation at more than 27,000 sites in placenta and cord blood using Illumina Methylation Assay. In addition, using Illumina Infinium High-Density DNA array we analyzed gene regulation of 48,000 mRNA in children conceived in vitro and in vivo. The objective of this study is to find out whether the gene regulation is affected by the methylation of the same gene (cis-affected) or other genes (trans-affected). It has been hypothesized in literature that gene expression level is most likely affected by cis methylation, but the results of our project revealed that most of the gene expressions are trans-methylation affected. These findings were deduced by measuring the correlation between methylation and gene expression for 23 samples. In addition, a permutation test is used to assess the significance of the correlation.

Discovering Predictive Markers of Birth Weight

In another project with Dr. Carmen Sapienza we analyzed the association between Assisted Reproduction Technologies (ART) and low birth weight, likely to become of increasing concern as the ART population ages. We have examined epidemiological data (DNA methylation level) at more than 700 loci selected for perceived importance in embryonic development or likelihood

of transcriptional imprinting to identify epigenetic differences that are correlated with birth weight from placenta and cord blood tissues of 22 samples. We identified 6 candidate loci, two from blood (APOE, MSX1) and four from placenta (GRB10c, PGRMC1, RGS14, SHMT2), whose methylation explain about 78% of the variance of birth weight. To that end, a lasso regularized linear regression was used first with the objective of finding the marginal effects of consistent gene methylation on birth weight using leave-one-out cross validation. The candidate genes methylation selected in the first stage were used to build an additive and interaction model aimed to find out the putative gene-gene methylation interactions.

Characterizing Domperidone Side-Effects by Genome-Wide Association Analysis

In collaboration with Dr. Henry Parkman from the Gastroenterology Section of the Department of Medicine at Temple Medical School, and Dr. Michael Jacob and Dr. Evgeny Krynetskiy from School of Pharmacy we have conducted large scale data analysis aimed to select relevant SNPs from the DNA microarray experiments in order to develop a strategy for rational selection of patients for domperidone therapy. In this project DNA samples extracted from the saliva of 46 patients treated with domperidone were analyzed using Affymetrix 6.0 SNP microarrays. Non-genetic parameters including demographics and therapeutic outcome (effectiveness and side effects) were also recorded. Data analysis was performed to determine association between genotype and side effects of domperidone.

Our analysis consisted of L1 regularized logistic regression followed by a wrapper based classification with forward feature selection in a pool of non-zero SNPs selected in the first stage analysis. In cross-correlation experiments we found that 24 SNPs were consistently highly correlated with the response to drug side effects. Genetic polymorphisms in ATF1, MPRIP, CACNB2, KRT8, and NPSR1 genes were found to significantly correlate with side effects of domperidone. Ubiquitin mediated proteolysis (UBE2E2, UBE2E1, UBE3A), cardiac muscle contraction (CACNB2) are also related. As alternative techniques, false discovery rate control method and correlation based feature selection method were also used to select relevant SNPs. The findings by these alternatives overlap with SNP list generated by L1 regularized logistic regression method, suggesting that SNP selected through the performed data analysis are stable.

In addition, we also identified the subsets of SNPs which show the most interactions to predict the target value. We developed a simple predictor model based on only 3 SNPs that in 10-fold cross validation was 100% accurate in predicting drug side effects.

We have published an abstract on this finding at a conference and are currently preparing a full manuscript for submission.

Genome-Wise Screening of Stress Conditions in COPD

Most recently we started a new collaboration with Dr. Steven Kelsen from the Pulmonary Section of the Department of Medicine at Temple Medical School, and Dr. Madesh Muniswamy from Department of Biochemistry. We performed analysis of a genome-wide screening experiment in which cells in vitro were subjected to simulated stress conditions that could lead to COPD. In these experiments the majority of cells die due to stress, while some of them survive

for longer period. The goal of the experiment is to find which genes are responsible for the survival of those cells. In the preliminary analysis, we searched for metabolic pathways that contain several of these genes and could possibly explain the process that leads to the survival of the cells. Gene ZNF217 has been identified as very important in the process, but the mechanism of its interaction with other genes has not yet been clearly identified. We assisted Dr. Kelsen's and Dr. Muniswamy's group in finding possible ZNF217 interactions by performing genome wide searches for possible binding sites of ZNF217.

We also conducted an initial signaling pathway assay for discovered genes. In a preliminary analysis we found that CCNA1 is linked to acute myeloid leukemia, cell cycle and cancer; ADA is associated with primary immunodeficiency; NOX3 is associated with leukocyte transendothelial migration; NCR1 is related to natural killer cell mediated cytotoxicity.

Research Project 21: Project Title and Purpose

Neuroimaging of Dextroamphetamine Effects in Aphasia - Aphasia is a neurological disorder characterized by a loss of the ability to understand or produce speech that occurs when language areas of the brain are damaged. The main treatment for the disorder has traditionally been speech and language therapy. However, recent studies have suggested that the outcome of this therapy can be significantly enhanced with the use of a particular medication called dextroamphetamine. The purpose of this project is to use an advanced brain imaging technique (fMRI) to examine the influence of this medication on brain activity while individuals with aphasia are engaged in tasks requiring speech processing. This type of assessment will facilitate an understanding of the nature of the positive treatment effects that have been described and may eventually allow us to predict which patients are likely to benefit from this form of adjuvant treatment.

Anticipated Duration of Project

9/9/2009 - 6/30/2011

Project Overview

Aphasia is an acquired communication disorder in which a person's ability to produce and/or comprehend language is impaired due to damage to neural systems that mediate the processing of speech. Aphasia affects more than 1 million Americans, with 80,000 new cases each year from stroke alone. Speech/language therapy is the traditional form of treatment for the disorder. However, recent neuropharmacologic studies have suggested that the outcome of speech/language therapy in patients with aphasia can be enhanced by adjuvant treatment with low doses of the medication dextroamphetamine (D-AMPH). The nature of this effect and its neurophysiological correlates remain unspecified. This project therefore proposes to use functional magnetic resonance imaging (fMRI) to evaluate the effects of D-AMPH in stroke patients with aphasia. This technique examines changes in brain activity that occur when participants are engaged in cognitive tasks. We aim to test the hypothesis that a low dose of D-AMPH used in previous neuropharmacologic studies of aphasia results in increased brain activation in the left hemisphere during processing of speech. In order to test this, we will develop a protocol that is suitable for patients with aphasia to perform in the scanner

environment. We will then examine the effects of D-AMPH and placebo on cerebral activation indexed by fMRI and on behavioral responses recorded during performance of tasks requiring speech-processing. We propose to evaluate whether fMRI is sensitive to changes in cognitive processing in individual patients that result from administration of low doses of D-AMPH.

Principal Investigator

Gerry A. Stefanatos, DPhil
Associate Professor
Temple University
Department of Communication Sciences and Disorders
1701 N. 13th St.
Philadelphia, PA 19122

Other Participating Researchers

Feroze Mohammed, PhD, Ian Maitin, MD - employed by Temple University

Expected Research Outcomes and Benefits

Aphasia is a disorder of the ability to produce and/or comprehend language that occurs when language areas of the brain are damaged. The disorder affects more than 1 million Americans, with 80,000 new cases each year from stroke alone. It is associated with profound personal, economic and social implications and aphasia is consistently cited as one of the primary determinants of diminished quality of life in stroke survivors. Speech/language therapy is the primary treatment and can result in significant improvements over time. Medications have traditionally had little to no effect on the outcome of this disorder. However, recent studies have suggested that low doses of dextroamphetamine (D-AMPH), a medication typically used to treat attention deficits, can significantly improve outcome of speech/language therapy. It has been suggested that this combination of behavioral/medical treatment enhances the brain's ability to reorganize functions related to language, thus enhancing long-term outcome. However, treatment is not beneficial to all patients and the nature of the effect is not well understood. A better understanding of the mechanisms involved in the treatment effect would allow a more rational approach to prescribing this form of treatment. This project proposes to utilize an advanced brain imaging technique, functional magnetic resonance imaging (fMRI), to evaluate the influence of low dose D-AMPH on brain activation during speech processing in patients with aphasia. This controlled assessment of D-AMPH's effects will help elucidate its influence on brain function in patients with aphasia and provide a better understanding of the nature of the positive treatment effects that have been described when it is used in combination with speech/language therapy. The use of fMRI may potentially be developed as a highly efficient approach to examine medication effects and in predicting which patients are likely to benefit from this form of adjuvant treatment. If successful, this approach could potentially accelerate progress in clinical trials and research in aphasia.

Summary of Research Completed

In order to conduct this study at Temple University, it was necessary to establish an infrastructure of personnel and processes across departments that had not previously existed. While an established mechanism was in place to conduct clinical trials within the Temple University Hospital, there was no mechanism to allow an outpatient study. Therefore, in order to engage a protocol pharmacist to dispense the drug and maintain blindness, special arrangements needed to be established with the Department of Pharmacy Practice at the Temple University School of Pharmacy and the Outpatient Pharmacy at Temple University Hospital (TUH) to permit the dispensing of a controlled drug to patients involved in the protocol. The establishment of this relationship required discussions with the research pharmacist at Temple University Hospital, the assistant director, hospital counsel, and the Office of Clinical Trials. This relationship was eventually established and a process put in place. It was also necessary for us to submit an investigational new drug (IND) exemption request to the Food and Drug Administration.

In addition, significant time and energy was required to develop and institute the fMRI protocol to be used in the evaluation of drug effects in this double-blind placebo-controlled protocol. The protocol was to be run on the new three Tesla magnet located at TUH. At this point, the magnet is used clinically as well as for research. A procedure had to be established to allow non hospital research patients to be scheduled on the magnet, since existing scheduling systems were designed for patient use only. This required discussions with Radiology and the Temple University Institutional Review Board. In addition, a number of technical hurdles were addressed in utilizing research based protocols on the magnet. Hardware had to be purchased to allow triggers from the magnet to be acquired by experimental control software that is programmed to present stimuli and collect responses. In order to synchronize events on the magnet with events in the software controlling the experiment, a fiber optic response package was purchased from Current Designs in Philadelphia. This hardware converts the magnet's fiber optic signals to an electrical impulse and subsequently delivers the impulse, as a keyboard button press, to a laptop running experimentation software, allowing it to utilize the signal. We also had to make a number of substantial modifications to the stimulus delivery systems, including improved coupling of electrostatic earbuds to the ear canals. After evaluating a number of solutions, we found that modifying commercially-available in-the-ear gel-inserts designed for cell phone users allowed tight insertion of the Stax electrostatic earbuds. Because we were using Temple's new magnet, we had to utilize ear-defenders with a slim profile that would fit within the Siemens Verio bird-cage head coil.

Finally, we instituted a method to recruit patients for the protocol. We sent letters to local health care facilities involved in the treatment of individuals with aphasia. This included but was not limited to the University of Pennsylvania, Thomas Jefferson University Hospital, McGee Rehabilitation Institute, Abington Hospital, Episcopal Hospital, Mercy Hospital and a neighboring Temple aphasia lab among others. In addition, we have distributed informational pamphlets at specific geographic locations and have submitted advertisements to Craigslist. We also instituted a protocol for recruitment of patients being seen at Temple University Hospital through the Department of Physical Medicine & Rehabilitation.

After a thorough review of the scientific literature, we were unable to locate a satisfactory task to examine overall language function using fMRI in people with aphasia in a valid and reliable

manner. For instance, some robust tasks required reading, a skill which people with aphasia may lose entirely. Other tasks required the passive viewing of stimuli. This was not acceptable to us as we could not be sure of the extent to which a patient with aphasia may perform the task within the magnet environment with the attendant high intensity (~120-130 dB) scanner noise to compete for their attention.

Therefore, to achieve the most valid MRI activation possible, we developed a new task that allows the examination of language function in people with language deficits and allows the monitoring of participation by requiring a behavioral response. The task involves the simultaneous delivery of a visual and an auditory stimulus in contrasting linguistic and nonlinguistic conditions. In the linguistic condition, a subject views a simple scene with objects or people and hears a short sentence describing the scene. Half of the time the auditory sentence accurately describes the scene and half of the time the sentence inaccurately describes the scene. When the sentence does not match the scene a subject is required to click a mouse button. In the nonlinguistic condition a subject hears a combination of high or low tones, which are 150 ms sine waves at either 500 or 750 Hz with an inter-tone-interval of 350 ms. Simultaneously the subject is shown a series of four or five red circles on the screen, each connect to its two neighbors by a line. Each circle may occupy a 'high' position or 'low' position, creating a visual representation of what they are hearing. Half of the tone sequences they hear match what they are shown visually, while half do not match. When the visual and auditory stimuli do not match the subject is required to click a mouse button. This nonlinguistic control condition is matched in every way to the experimental condition except the linguistic nature of the stimuli.

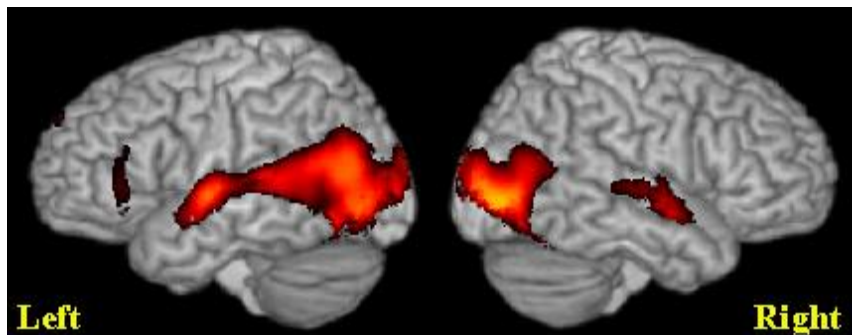
To evaluate the validity of our new task, we piloted it on student volunteers. The results of this pilot work were presented in October at the first annual Neurobiology of Language conference in Chicago. We found consistent activation of traditional left hemisphere auditory and language regions including superior temporal gyrus which extended anteriorly to temporal polar regions and posteriorly to angular gyrus. Substantial activation left hemisphere asymmetries were evident in the IFG, SMG, and AG, as would be expected in neurologically intact right-handed participants. The functional asymmetries revealed by our task showed a high pair-wise correlation with handedness as measured by the Edinburgh Handedness Inventory and with the results of dichotic listening, a behavioral measure of cerebral dominance. Figure 1 below shows the group data of activations in response to the sentence processing task and Figure 2 illustrates the conjunction of this activation among 12 or more participants. Figures 3a, b and c illustrate the activations elicited on the same task in a participant with aphasia. On one week, the participant was on a placebo while in the other week she was on a low dose of D-AMPH. There appear to be differences between weeks 1 and 2. We have not been unblinded as to treatment order so we cannot ascertain whether these difference represent an effect of the pharmacologic treatment.

In order to examine the effects of D-AMPH on working memory and continuous attention in the MR environment we incorporated three “n-back” tasks. These tasks require a participant to listen to a list of animal names. For each animal name, they need to determine whether it is the same as the animal name *n* items ago. That is, in the 2-back task, they must click the mouse button when the item they just heard is the same as 2 items ago. In the 1-back they need to press a button if the animal name they hear is the same as the previous animal name. Finally, in the 0-back task they need to click a mouse button if the animal name they just heard is the one they were instructed to listen for at the beginning of the task.

Each task underwent at least one round of revision in early-testing. For example, we piloted two versions of each of the n-back tasks in healthy college students to decide whether it was preferable to have them respond to each item (i.e. targets and nontargets) or to just indicate targets. At first we decided to have participants respond to both targets and non-targets. However, we found that some subjects with aphasia perform poorly if they are required to press one response button when they hear a target and another when they hear a non-target. Due to executive problems that often accompany aphasia, their performance is better when they are asked to press to a target and refrain from pressing to non-targets. Each fMRI task was modified to accommodate this change.

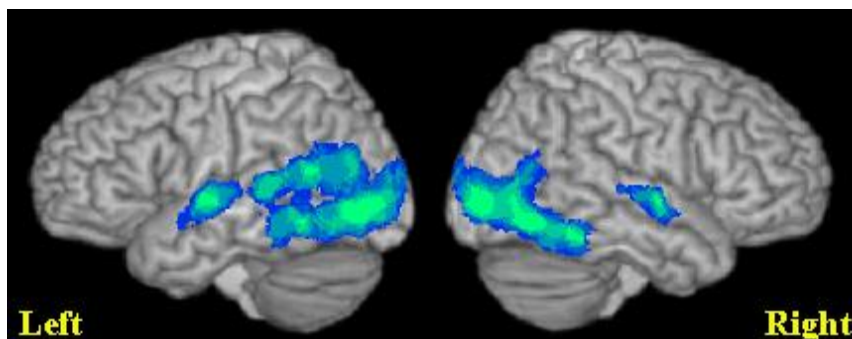
At this point in time we have identified and contacted 9 candidates for the study. Of these 9, two never enrolled, two did not pass the behavioral evaluation because of recovery from aphasia, two are expected to enroll pending their evaluations, and three patients are currently enrolled in the study. The project is at a data collection phase, and we will actively keep recruiting and interviewing patients who meet our preliminary inclusion criteria.

Figure 1.



Legend: Group activation maps revealed a strong left hemisphere asymmetry. Sentence processing activated traditional left hemisphere perisylvian auditory and language regions including superior temporal gyrus (BA 22 & 41) and transverse temporal gyrus, extending anteriorly to temporal polar regions, posteriorly to angular gyrus and ventrally to middle temporal gyrus. Activation of perisylvian cortex in the right hemisphere was more limited. Bilateral activations were evident in fusiform gyrus, extending posteriorly to visual cortex.

Figure 2.



Legend: Conjunction maps revealed high consistency of activation between subjects on the sentence processing task. The areas highlighted in blue-green represent activation present in 12 or more participants.

Figure 3

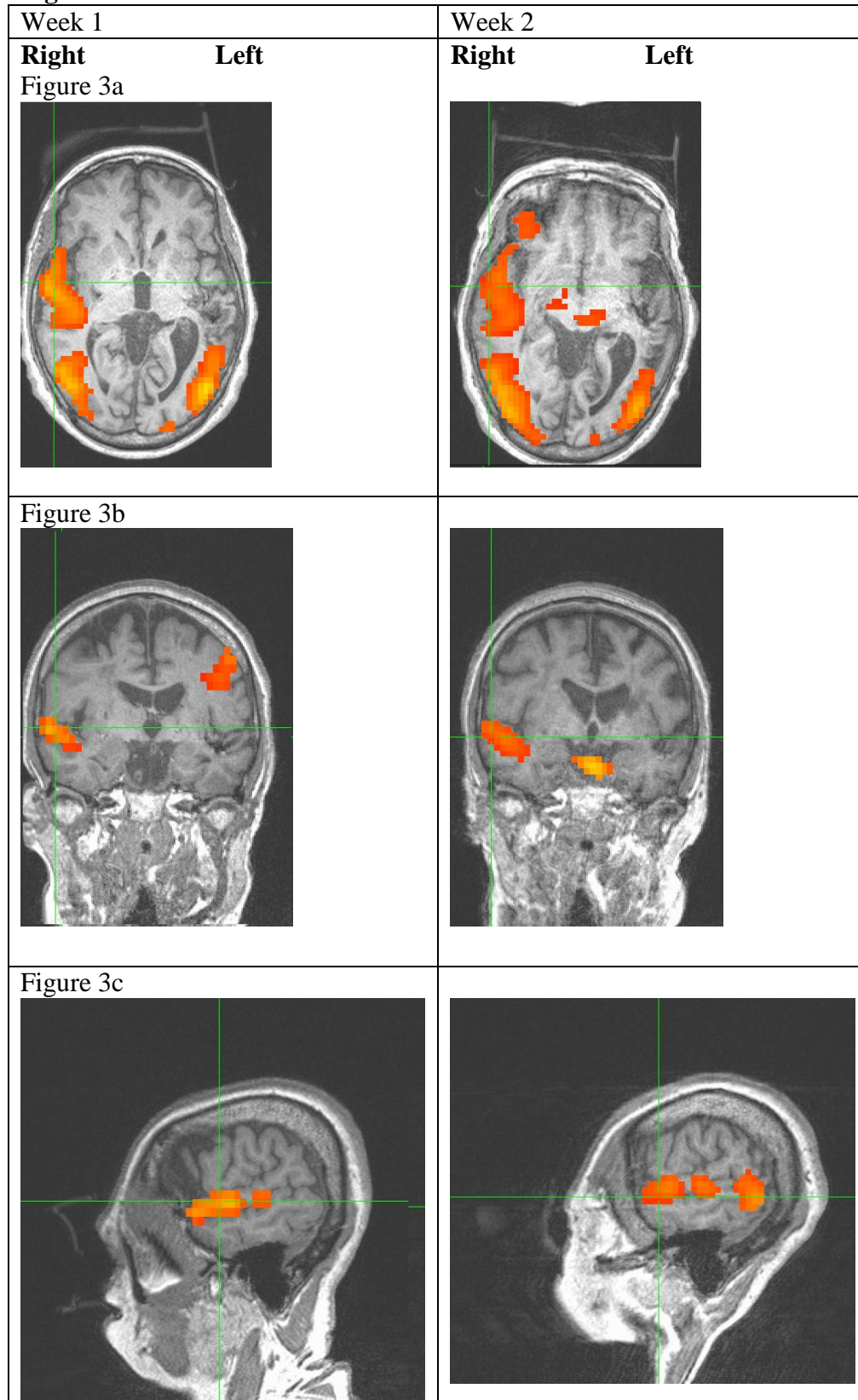


Figure 3a represents an axial view of activations elicited by the sentence comprehension task in a participant with aphasia. Note the marked absence of activation in the left cerebral hemisphere.

Figure 3b demonstrates a coronal view of the same activation.

Figure 3c demonstrates a lateral perspective on this activation. Note activation is more extensive in temporal lobe during week two compared to week one.